PLOS CLIMATE

RESEARCH ARTICLE

Downscaled seasonal forecasts for the California Current System: Skill assessment and prospects for living marine resource applications

Michael G. Jacox[1,2,3]*, Mercedes Pozo Buil[1,3], Stephanie Brodie[1,3], Michael A. Alexander[2], Dillon J. Amaya[2], Steven J. Bograd[1,3], Christopher A. Edwards[4], Jerome Fiechter[4], Elliott L. Hazen[1,3], Gaelle Hervieux[2,5], Desiree Tommasi[3,6]

1 Environmental Research Division, NOAA Southwest Fisheries Science Center, Monterey, California, United States of America, **2** Physical Sciences Division, NOAA Earth System Research Laboratories, Boulder, Colorado, United States of America, **3** Institute of Marine Sciences, University of California Santa Cruz, Santa Cruz, California, United States of America, **4** Ocean Sciences Department, University of California Santa Cruz, Santa Cruz, California, United States of America, **5** Cooperative Institute for Research in Environmental Sciences, University of Colorado, Boulder, Colorado, United States of America, **6** Fisheries Resources Division, NOAA Southwest Fisheries Science Center, La Jolla, California, United States of America

* michael.jacox@noaa.gov

Citation: Jacox MG, Buil MP, Brodie S, Alexander MA, Amaya DJ, Bograd SJ, et al. (2023) Downscaled seasonal forecasts for the California Current System: Skill assessment and prospects for living marine resource applications. PLOS Clim 2(10): e0000245. https://doi.org/10.1371/journal.pclm.0000245

Editor: Liqiang Xu, Hefei University of Technology, CHINA

Received: March 14, 2023

Accepted: September 9, 2023

Published: October 31, 2023

Peer Review History: PLOS recognizes the benefits of transparency in the peer review process; therefore, we enable the publication of all of the content of peer review and author responses alongside final, published articles. The editorial history of this article is available here: https://doi.org/10.1371/journal.pclm.0000245

Data Availability Statement: Output from the UCSC CCS reanalysis is available from https://oceanmodeling.ucsc.edu. Shore station SST data

Abstract

Ocean forecasting is now widely recognized as an important approach to improve the resilience of marine ecosystems, coastal communities, and economies to climate variability and change. In particular, regionally tailored forecasts may serve as the foundation for a wide range of applications to facilitate proactive decision making. Here, we describe and assess ~30 years of retrospective seasonal (1–12 month) forecasts for the California Current System, produced by forcing a regional ocean model with output from a global forecast system. Considerable forecast skill is evident for surface and bottom temperatures, sea surface height, and upper ocean stratification. In contrast, mixed layer depth, surface wind stress, and surface currents exhibit little predictability. Ocean conditions tend to be more predictable in the first half of the year, owing to greater persistence for forecasts initialized in winter and dynamical forecast skill consistent with winter/spring influence of the El Niño–Southern Oscillation (ENSO) for forecasts initialized in summer. Forecast skill above persistence appears to come through the ocean more than through the atmosphere. We also test the sensitivity of forecast performance to downscaling method; bias correcting global model output before running the regional model greatly reduces bias in the downscaled forecasts, but only marginally improves prediction of interannual variability. We then tailor the physical forecast evaluation to a suite of potential ecological applications, including species distribution and recruitment, bycatch and ship-strike risk, and indicators of ecosystem change. This evaluation serves as a template for identifying promising ecological forecasts based on the physical parameters that underlie them. Finally, we discuss suggestions for developing operational forecast products, including methodological considerations for downscaling as well as the respective roles of regional and global forecasts.

were obtained from https://shorestations.ucsd.edu/publications/data/. Tide gauge data were obtained from the University of Hawaii Sea Level Center (https://uhslc.soest.hawaii.edu/datainfo/). NOAA OISST v2.1 data were obtained from NOAA's Physical Sciences Laboratory (https://psl.noaa.gov/data/gridded/data.noaa.oisst.v2.highres.html). Data and code to reproduce figures are available at https://github.com/mjacox/PLOSClimate_2023.

Funding: Funding support was provided by the National Oceanic and Atmospheric Administration (NOAA) Modeling, Analysis, Prediction, and Projection (MAPP) program and the NOAA Fisheries Office of Science and Technology.

Competing interests: The authors have declared that no competing interests exist.

1. Introduction

The need for proactive ocean decision making is now well established, as the impacts of climate variability–especially extreme events–highlight the limitations of static management strategies. In the U.S., for example, myriad ecological, social, and economic impacts of ocean variability over the past decade have motivated a growing push to incorporate forward-looking environmental information in the management of coastal communities, fisheries, and marine protected areas [1, 2]. To that end, seasonal (1–12 month) ocean forecasts have an important role to play when managing marine resources in a changing climate [3], filling a critical gap between real-time information and long-term outlooks. For example, seasonal forecasts have the potential to inform decisions on fish catch limits, timing of fishery closures, and allocation of monitoring resources [4], and past work has highlighted both the promise and challenges of marine ecosystem prediction on seasonal timescales [4–6].

A logical approach to creating marine ecosystem forecasts is to start from skillful physical climate forecasts, which are then connected by statistical or mechanistic models to ecological targets of interest. In this construction, a wide variety of ecological models developed for retrospective or near-real-time application could be readily transitioned to forecast mode (e.g., Section 3.4). The physical predictions can be global or regional in scale, but while global climate forecasts are widely available, oceanographic output from these models is often limited to few surface variables, predominantly sea surface temperature (SST) [7]. Furthermore, there is a desire for predictions of fine-scale features and processes that are relevant to marine resource management but are not resolved by global forecast systems. Dynamical downscaling allows for regionally tailored models with relatively high resolution, and the downscaling process can also be used to correct for regional biases in global models. As a result, dynamical downscaling has been widely used to produce regional ocean projections under climate change [8]. However, examples of dynamically downscaled seasonal forecasts and assessments of their forecast skill are less common [though see 9, 10].

One region for which downscaled seasonal forecasts hold interest and potential is the California Current System (CCS), running along the west coast of North America. As one of the world's major eastern boundary upwelling systems, the CCS supports a highly productive marine biome and human activities including socio-economically important fisheries and tourism [11]. The physical, chemical, and biological environment of the CCS exhibits considerable variability on subseasonal, seasonal, and interannual timescales [12], with notable ecological disruptions arising from climate anomalies including delayed upwelling [13], ENSO events [14 and references therein], and other marine heatwaves [15]. Importantly, largely due to the influence of ENSO, the CCS is one of the more predictable areas of the ocean, especially among extratropical regions [16, 17].

Here, we present a ~30-year retrospective skill assessment for the first downscaled seasonal forecasts spanning the U.S. portion of the California Current System (CCS) and extending ~1000 km offshore. In doing so, our aims are to (i) evaluate forecast skill for coastal and offshore conditions in the CCS, including for metrics of vertical water column structure that have rarely (if ever) been evaluated in ocean predictions, (ii) demonstrate a framework for using physical forecast skill assessment as a key step toward identifying ecological forecasts that are poised to be skillful, and (iii) provide insight for developing operational forecast products, including methodological considerations and the role of regional vs. global forecasts.

2. Methods

2.1. Forecast system

2.1.1. Forecast system overview. The regional ocean forecast system employed here consists of a regional ocean model (Fig 1) forced by output from a global climate forecast system. In order to thoroughly evaluate the performance of the system, we have run a set of retrospective forecasts (reforecasts) spanning approximately three decades (1982–2010). Details of the forecast system, including the global climate forecasts, the regional ocean model, and the downscaling procedure, are described below.

2.1.2. Global climate forecast system. Surface forcing and lateral ocean boundary conditions for the downscaled forecasts were derived from the fourth version of the Canadian Center for Climate Modeling Analysis's coupled climate model (hereafter CanCM4 [18]). Forecasts were initialized every month, with each forecast extending 12 months into the future (i.e., with lead times up to 12 months). To capture uncertainty due to internal climate variability, each forecast includes 10 ensemble members initialized from separate data assimilation runs such that their initial conditions are slightly different [18]. CanCM4 output is available for all atmospheric and oceanic variables needed to force the regional ocean model over the 1982–2010 period; surface atmospheric conditions and radiative forcing are available at daily frequency, while three-dimensional ocean boundary conditions are available as monthly averages. CanCM4 is one of the models in the North American Multimodel Ensemble (NMME [19]), and has been shown to exhibit considerable forecast skill for SST in the CCS [20]. Other global climate forecast systems exhibit similar patterns in skill to those of CanCM4 [17, 20],

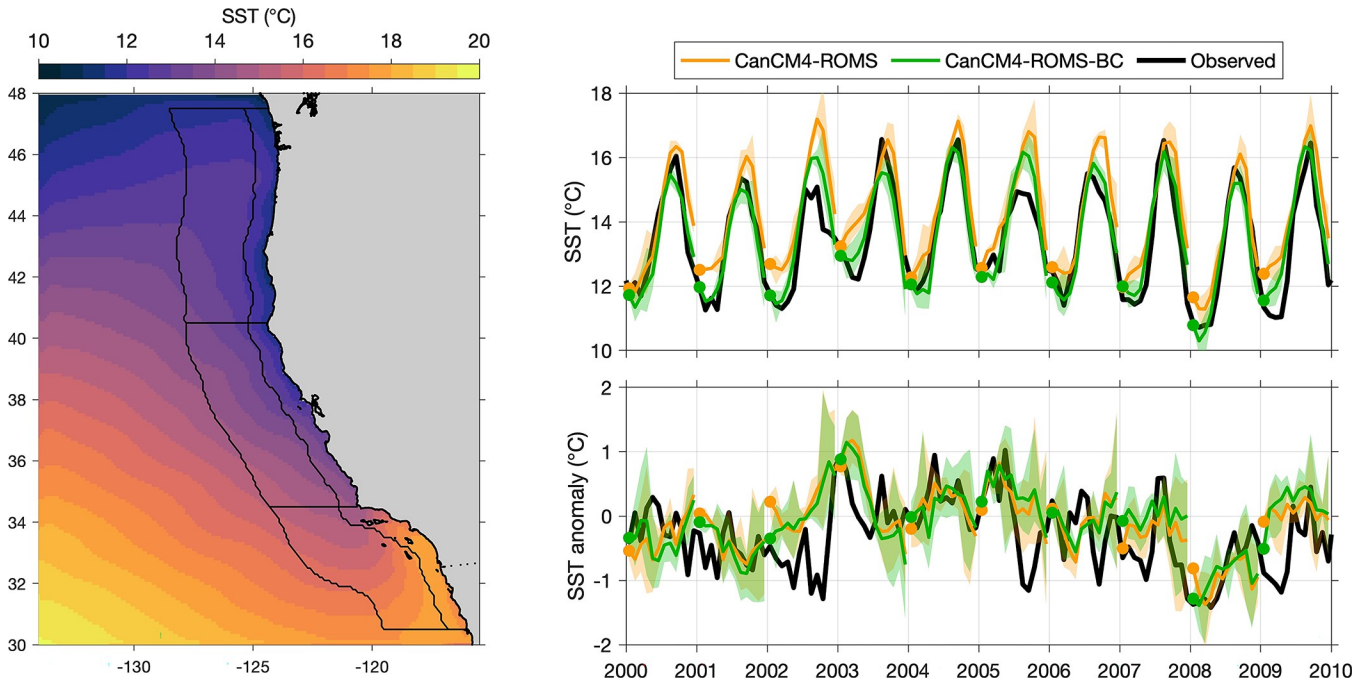

Fig 1. Sample forecast output. (left) California Current System ROMS domain, with color indicating mean SST for the 1982–2010 period of the study. Black contours indicate 75 and 300 km from shore, as well as divisions between north, central, and south regions. (right) Output from downscaled forecasts for (top) SST and (bottom) SST anomaly averaged within the 75 km coastal band outlined on the map. Forecast conditions are shown for two sets of downscaled runs, which differ in whether the forcing derived from the CanCM4 global models was bias corrected (CanCM4-ROMS-BC) or not (CanCM4-ROMS) prior to downscaling. The forecast initialization (colored circles), ensemble mean (colored lines) and ensemble spread (colored shading) are shown for each forecast, with observed conditions in black. For clarity, only forecasts initialized in January for 2000–2009 are shown.

https://doi.org/10.1371/journal.pclm.0000245.g001

and for seasonal forecasts the intramodel spread is much larger than the intermodel spread [e.g., 21], so we ran multiple ensemble members from CanCM4 rather than running members from multiple models.

2.1.3. Regional ocean model. Forecasts were dynamically downscaled using a CCS configuration of the Regional Ocean Modeling System (ROMS), covering the U.S. west coast and extending ~1000 km offshore (30–48˚N, 134–115.5˚W). Model resolution is 0.1 degrees (~7–11 km) in the horizontal, with 42 terrain-following levels in the vertical [22]. This model and its variants have been used extensively to evaluate the CCS physical and biogeochemical ocean state [23–25], its variability and response to climate forcing [26–28], and its influence on marine biological communities ranging from phytoplankton to top predators [29–32].

2.1.4. Regional ocean model forcing and initialization. Due to computational constraints, the full suite of global climate forecasts (12 forecasts per year, 10 ensemble members) was reduced to a smaller subset for dynamical downscaling. To capture seasonal differences in predictability, we downscaled forecasts initialized in January and July, and three ensemble members were downscaled for each forecast. A three-member ensemble was chosen to balance the computational and storage costs of running additional members with the diminishing returns of skill improvement as the ensemble gets larger [6]. For each forecast, we used ensemble members 2, 8, and 10 in the CanCM4 output. When treated as independent forecasts these three ensemble members exhibit relatively low, moderate, and high retrospective SST forecast skill in the CCS, giving us forecasts that are representative of what should be expected from a typical 3-member ensemble (S1 Fig).

ROMS forcing fields were derived from the CanCM4 global forecasts in two ways: one in which CanCM4 fields were interpolated directly to the ROMS grid (denoted CanCM4-ROMS), and one in which the CanCM4 fields were bias corrected before being used as forcing for ROMS (denoted CanCM4-ROMS-BC). In the latter case, the bias-corrected forcing was constructed by (i) subtracting the initialization- and lead time-dependent climatology from CanCM4 forecast fields to obtain CanCM4 forecast anomalies [as in 16], and then (ii) adding the low-resolution CanCM4 anomalies to high resolution 1982–2010 climatologies of the surface and ocean boundary conditions, obtained from the European Centre for Medium-Range Weather Forecasts (ECMWF) version 5 atmospheric reanalysis (ERA5 [33]) and the Simple Ocean Data Assimilation version 2.1.6 (SODA [34]), respectively. For this second step, surface CanCM4 anomalies from the ocean point closest to land were extended over land (i.e., the land was flooded) to avoid artifacts associated with the land-sea interface during interpolation, and then bicubic interpolation was used to put CanCM4 anomalies on the higher resolution grid.

Initialization was also handled differently between the two forecast configurations. In CanCM4-ROMS, the ocean initial conditions were interpolated directly from CanCM4 output. Since CanCM4 ocean fields were provided as monthly averages, the initial condition was obtained by averaging the zero-lead forecasts for the two months surrounding the initialization date. For example, the initial condition for the Jan. 1, 2000 forecast was obtained by averaging the December conditions from the December 1999 forecast and the January conditions from the January 2000 forecast (note that in a true forecast mode, the global model should supply initial conditions from the beginning of the month). In CanCM4-ROMS-BC, the initial condition was obtained from the UC Santa Cruz CCS ocean reanalysis ([35]; Section 2.2.2). Using the historical reanalysis to initialize retrospective forecasts simulates an approach in which operational forecasts are initialized from a near-real-time regional analysis available for the CCS (oceanmodeling.ucsc.edu/ccsnrt, version 2016a).

Given the different configurations of their initialization and forcing, CanCM4-ROMS and CanCM4-ROMS-BC represent opposite ends of the spectrum for regional tailoring of the

downscaled forecasts; CanCM4-ROMS is forced solely by the global forecast output while CanCM4-ROMS-BC relies on high resolution atmosphere and ocean reanalyses to construct both the initial condition and the forcing. While we focus on CanCM4-ROMS-BC to quantify the potential skill of a CCS seasonal forecast system, comparison between the two configurations (Section 3.3) provides insight into the added value of bias-correcting the forcing and using a near-real-time regional ocean analysis for forecast initialization, both of which are non-trivial additions to the workflow.

2.2. Skill assessment

2.2.1. Variables assessed. Forecast skill was evaluated for a suite of atmospheric and oceanic variables. In the atmosphere, we examined surface wind stress in the eastward and northward directions (*sustr* and *svstr*, respectively) as well as wind stress curl (*curl*). At the ocean surface, we examined sea surface temperature (*SST*), sea surface height (*SSH*), and surface currents in the eastward and northward directions (*su* and *sv*, respectively). The upper ocean water column structure was characterized by the mixed layer depth (*MLD*), defined by a density change corresponding with a 0.8˚C temperature deviation [36], and the buoyancy frequency (*BF*; a measure of stratification) averaged over the upper 200m. Lastly, bottom temperature (*BT*) was included for its importance to benthic species, with a focus on the nearshore environment where bottom depth is less than ~1000 m. These variables were chosen for their potential as predictors of variability in the distributions and populations of marine species ranging from phytoplankton and krill [37, 38] to fish, sharks, and top predators [30, 39]. Monthly averages of all variables were computed for skill assessment.

2.2.2. Verification data. Forecast skill was evaluated using ocean reanalyses, satellite observations, and several in situ data sets. The UC Santa Cruz CCS reanalysis (CCSRA [35]) is based on the same ROMS model domain described in Section 2.1.3, though with different atmosphere and ocean boundary forcing. This reanalysis spans 1980–2010 and assimilates satellite SST and SSH data as well as available *in situ* salinity and temperature data. As a verification data set, CCSRA has the advantages of matching the domain and resolution of the downscaled forecasts and resolving the full water column. Past analyses have shown that surface and water column properties of CCSRA compare favorably to observations from ship-based surveys, satellites, shore stations, underwater gliders, and Argo floats [35, 40, 41]. A second ocean reanalysis, the Global Ocean Reanalysis and Simulations (GLORYS) version 1 was also used as a separate verification data set. GLORYS has global coverage at 1/12 degree horizontal resolution with 50 vertical levels. GLORYS uses the Nucleus for European Modelling of the Ocean (NEMO) ocean model with surface forcing from the ECMWF ERA-Interim reanalysis, and is available for 1993–2019. Similar to CCSRA, GLORYS assimilates satellite SST and SSH observations as well as in situ temperature and salinity, and exhibits high fidelity to independent observations in the CCS [41, 42].

Additional SST measurements for verification were taken from version 2.1 of NOAA's daily 0.25˚ resolution Optimum Interpolation SST product (OISST [43, 44]) as well as shore-based observations maintained by a network of institutions along the U.S. west coast (https://shorestations.ucsd.edu). Focusing on locations with comprehensive coverage for the 1982–2010 forecast verification period, we used data from four locations along the California coast: the Farallon Islands (37.7˚N), Pacific Grove (36.6˚N), Newport Beach (33.6˚N), and La Jolla (32.9˚N). Similarly, to evaluate SSH forecasts at coastal sites, tide gauge data were obtained from the University of Hawaii Sea Level Center (Caldwell et al. 2015) [45] for nine sites from Toke Point, WA (46.7˚N) to La Jolla, CA (32.9˚N). For model verification, shore station and tide gauge data were compared to the closest coastal grid cell in the model. For all verification

datasets, monthly averages were computed from daily data, and monthly anomalies were calculated by removing the 1982–2010 monthly climatology.

Lastly, we leverage a pre-existing set of regional ocean model runs to explore the relative contributions of atmospheric and oceanic forcing to forecast skill (see Section 4). In brief, the same forcing used to drive CCSRA was applied to a historical simulation without data assimilation. This run (referred to herein as a hindcast) differs slightly from CCSRA but captures much of the same variability due to the common forcing. The surface fluxes and ocean boundary conditions for the hindcast were then used to drive two additional runs: one with realistic wind forcing but climatological ocean boundary conditions (the "Wind" run) and one with realistic ocean boundary conditions but climatological wind forcing (the "Ocean" run). These runs, described in detail in [28], were designed to separate the influence of wind forcing over the regional domain from ocean forcing that comes through the lateral boundaries of the ocean model.

2.2.3. Skill metrics. Forecast skill is quantified using a suite of deterministic and probabilistic metrics that have been previously employed for climate forecast evaluation [17, 46]. Each metric is calculated across all forecast years (N = 29) for each initialization month and lead time. Bias, the mean difference between forecast and observed fields, is used to determine the ability of forecasts to represent the mean state. Anomaly correlation coefficient (*ACC*), the correlation between forecast and observed anomalies, is used to assess forecast skill for interannual variability. Forecast anomalies are calculated using a lead-dependent forecast climatology to account for model drift. The combined influence of errors in the forecast mean state and variability is quantified using the root mean squared difference (*RMSD*) of observed and forecast fields. Finally, forecast accuracy provides a probabilistic skill measure for categorical predictions. Here, the categories are terciles of each variable, such that forecast accuracy for a given initialization and lead time is the fraction of forecasts that correctly predicted whether an event (e.g., SST being in the upper tercile) would occur [47]. ACC varies between -1 and 1, with 1 being perfect and 0 being equal to chance. Forecast accuracy varies between 0 and 1, with 1 being perfect. For terciles, a random forecast is expected to give forecast accuracy of 0.56 (the random probability of a true positive plus the random probability of a true negative; ⅓*⅓ + ⅔*⅔). For bias and RMSD, smaller numbers are better.

As in previous forecast skill assessments (e.g., [16]), forecast skill is evaluated for significance using ACC. First, sample autocorrelation is accounted for by calculating the effective degrees of freedom (N_{eff}) as in [48]:

$$N_{eff} = \frac{N}{\sum_{\tau=0}^{N-1}\left(1-\frac{\tau}{N}\right) r_{\tau}^{F} r_{\tau}^{O}}$$

where N is the number of samples in the forecast time series, and r_{τ}^{F} and r_{τ}^{O} are autocorrelation coefficients for the forecast and observed time series, respectively, at lag τ. We then apply Fisher's z transformation to the Pearson correlation between forecast and observations ($r_{F,O}$):

$$Z_{F,O} = 0.5\ ln\left(\frac{1+r_{F,O}}{1-r_{F,O}}\right)$$

where $Z_{F,O}$ follows a z distribution with *Neff*– 3 degrees of freedom. We calculate 95% confidence bounds for $Z_{F,O}$ and then transform back to $r_{F,O}$; if the lower confidence bound is greater than zero, the forecast skill is significant. As a further benchmark against which model forecasts can be evaluated, we also calculate forecast skill for persistence forecasts, which assume that anomalies observed in the month prior to forecast initialization will persist throughout the forecast.

For each forecast, an ensemble mean forecast is calculated as the mean of the three ensemble members (Fig 1). The ensemble mean forecast is the main focus of our results (Section 3), with Section 3.2 discussing the characteristics of individual ensemble members.

2.3. Assessment of ecological forecast potential

As a first step toward assessing the broader applicability of the physical forecasts described here, we have identified a suite of potential ecological forecast applications in the California Current System (Table 1). In brief, they are (1) estimates of Pacific sardine spawning habitat and recruitment off Southern California [49, 50], (2) the Temperature Observations to Avoid Loggerheads (TOTAL) tool, designed to limit bycatch of Loggerhead turtles in the Southern California Bight [51], (3) the Habitat Compression Index (HCI), a measure of nearshore cold water habitat related to ecosystem changes and whale entanglement risk off central California [52, 53], (4) distribution of suitable albacore habitat off Oregon and Washington [54], (5) the Anchovy Ecosystem Indicator (AEI), an indicator of top predator foraging and reproduction off central California [55], (6) EcoCast, a tool designed to limit bycatch and promote sustainable fishing for swordfish in the California drift gillnet fishery [56], and (7) WhaleWatch, a tool to predict blue whale distributions and identify ship strike risk in the Southern California Bight [39, 57]. Note that this is a non-exhaustive list of potential applications that have not yet been implemented in a regional forecast framework. There are other west coast applications for which spatially-explicit forecast capability has been demonstrated, e.g., for Pacific sardine distribution [58], Pacific hake distribution [59], and Dungeness crab catch rates and megalopae occurrence [60, 61].

For each application, we identified the region, physical variables, and months of the year for which forecasts are needed (Table 1). For this purpose, each application is associated with one or more broad regions identified as north, central, and south, with divisions at Cape Mendocino (~40.5˚N) and Point Conception (~34.5˚N), each extending 300 km offshore (Fig 1). We then summarized the physical forecast skill given the requirements of each application, with the goal of providing an initial assessment of how likely they are to be successfully transitioned to a forecast framework (Section 3.4). Specifically, we collated ACCs for each variable/region/forecast month associated with a given application and then characterized the distribution of those ACCs. For example, in the case of sardine spawning habitat and recruitment, we consider the distribution of just six ACCs (one region–the Southern CCS, two variables–SST

Table 1. Prospects for living marine resource forecasts based on physical forecast skill. Key parameters for previously identified potential living marine resource forecast applications. Regions are divided into north (40.5–47.5N), central (34.5–40.5), and south (30.5–34.5), with each extending 300 km offshore (Fig 1). The "Full suite" of variables includes all of the variables assessed herein (e.g., Fig 2), with the exception of bottom temperature. The "Spatially explicit?" column denotes whether an application requires on spatially resolved data (Yes) or an average over a larger area (No).

Application	Region	Key physical variables	Target months	Spatially explicit?	References
Sardine spawning habitat and recruitment	South	SST, SSH	March–May	No	[49, 50]
Temperature Observations To Avoid Loggerheads (TOTAL; bycatch risk)	South	SST	December–July	No	[51]
Habitat Compression Index (HCI; whale entanglement risk)	Central	SST	March–November	Yes	[52, 53]
Albacore distribution	North	Full suite	June–November	Yes	[54]
Anchovy Ecosystem Indicator (AEI: top predator foraging and reproduction)	Central	Full suite	April–July	Yes	[55]
EcoCast (bycatch risk)	North, Central, South	Full suite	August–January	Yes	[56]
WhaleWatch (ship strike risk)	South	Full suite	May–November	Yes	[39, 57]

https://doi.org/10.1371/journal.pclm.0000245.t001

and SSH, and three forecast months–March, April, and May). On the other extreme, for EcoCast we consider the distribution of 180 ACCs (three regions, 10 variables, six forecast months). All forecasts are taken from the most recent initialization (i.e., forecasts of January–June are from the January initialization, forecasts of July–December are from the July initialization). For applications that rely on a large suite of variables, we also consider the skill for a smaller subset of variables that exhibit relatively high skill (SST, SSH, and buoyancy frequency). Since the forecasts do not include biogeochemistry, chlorophyll concentration is excluded from this analysis despite being included as a predictor in several of the applications.

3. Results

3.1. Forecast skill

For a coastal band along the U.S. west coast (i.e., within 75 km of shore), the physical variables evaluated here can be grouped into two broad categories: those that can be forecast skillfully at relatively long lead times of several months or more, and those for which significant forecast skill is limited to lead times less than three months (Fig 2). The former set of variables includes SSH, SST, bottom temperature, and to a lesser extent, upper ocean buoyancy frequency (stratification), while the latter includes mixed layer depth as well as surface wind stress and currents. Despite some spatial structure in forecast skill, the qualitative distinction between more and less skillful variables holds across the broader offshore area of the model domain (Fig 3, S2 and S3 Figs). Given that the atmosphere has much shorter decorrelation scales than the ocean, it is not surprising that there is limited seasonal forecast skill for surface wind variability, and by extension for mixed layer depth and surface currents, which are strongly driven by wind forcing. For these variables, a more thorough exploration of subseasonal (i.e., 45–60 day) forecasts is likely warranted, as there is a wide array of potential marine resource management applications on those shorter timescales [62]. For the remainder of this section, we focus on the variables that are more predictable on seasonal timescales.

In the nearshore zone, SSH is the most predictable of all variables evaluated here. When evaluated with the CCS ocean reanalysis, SSH forecasts exhibit significant skill at all lead times for both January and July initializations. For SST, bottom temperature, and stratification, forecast skill is dependent more on the time of year being predicted than on the time of year when forecasts are initialized; both January- and July-initialized forecasts exhibit elevated skill for predictions of winter and spring conditions. For the January forecasts this period is the first half of the forecast and much of the skill can be attributed to persistence of anomalies present at the time of initialization. In contrast, for forecasts initialized in July, skill in the winter-spring period (corresponding to lead times of >6 months) is significantly higher than that of a persistence forecast (Fig 2). Elevated skill from the dynamical forecasts in the winter/spring period is consistent with the influence of the El Niño-Southern Oscillation (ENSO), whose teleconnections represent a predictable signal impacting the CCS in the winter and spring following the peak of El Niño and La Niña events [20, 63]. The patterns in persistence forecast skill are consistent with mixed layer dynamics, where a deep winter mixed layer has greater thermal inertia than the shallow summer mixed layer. Persistence is much more pronounced for bottom temperature than for SST, with significant skill extending 9 months and 4 months for January- and July-initialized forecasts, respectively (compared to 5 months and 1 month for SST). This elevated skill for bottom conditions at lead times up to ~4 months was also noted by [9]. Additional mechanisms that may contribute to predictability along the U.S. west coast include advection and reemergence [6, 64, 65], though these mechanisms have not been assessed in ocean forecasts.

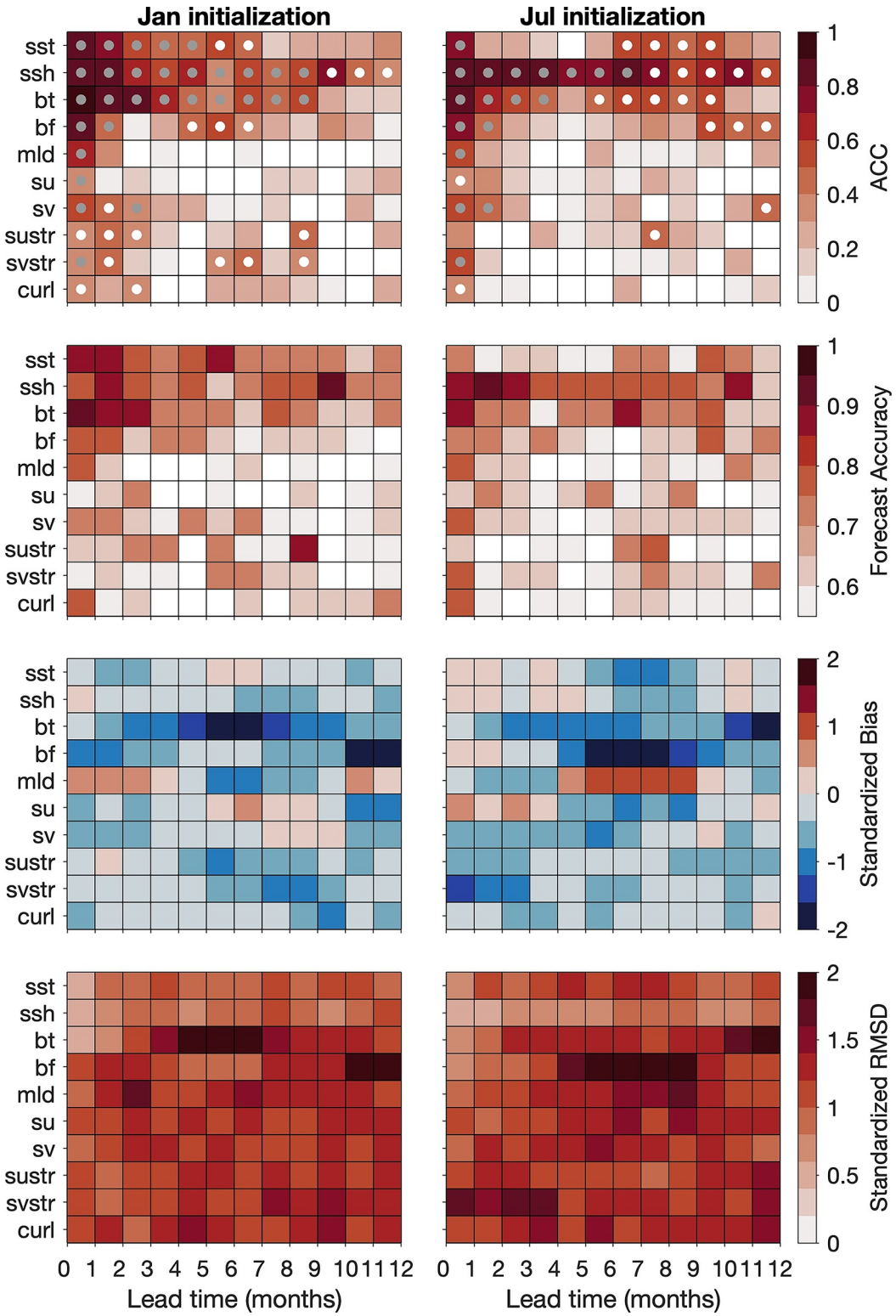

Fig 2. Skill summary for downscaled forecasts (ROMS-CanCM4-BC) initialized in (left) January and (right) July of each year, 1982–2010. Forecast skill is shown for conditions averaged over the 75 km coastal band shown in Fig 1, except bottom temperature, which is averaged to a maximum bottom depth of 1000 m. Four skill metrics are reported here: anomaly correlation coefficient (ACC), forecast accuracy, bias, and root mean square difference (RMSD). Bias and RMSD are standardized (i.e., divided by the standard deviation of anomalies across all years) to facilitate comparison between

variables on the same scale. For ACC, gray dots indicate model forecast skill that is significantly greater than zero (95% confidence), while white dots indicate model forecast skill that is significantly greater than zero when persistence forecast skill is not significantly greater than zero. Forecast accuracy is shown for the upper tercile of each variable. For ACC and forecast accuracy, skill below that of a random forecast (0 for ACC, 0.56 for forecast accuracy) is colored white. Variable abbreviations (top to bottom) are: sea surface temperature (sst), sea surface height (ssh), bottom temperature (bt), buoyancy frequency (bf), mixed layer depth (mld), surface eastward and northward current velocities (su, sv), surface eastward and northward wind stress (sustr, svstr), and wind stress curl (curl).

https://doi.org/10.1371/journal.pclm.0000245.g002

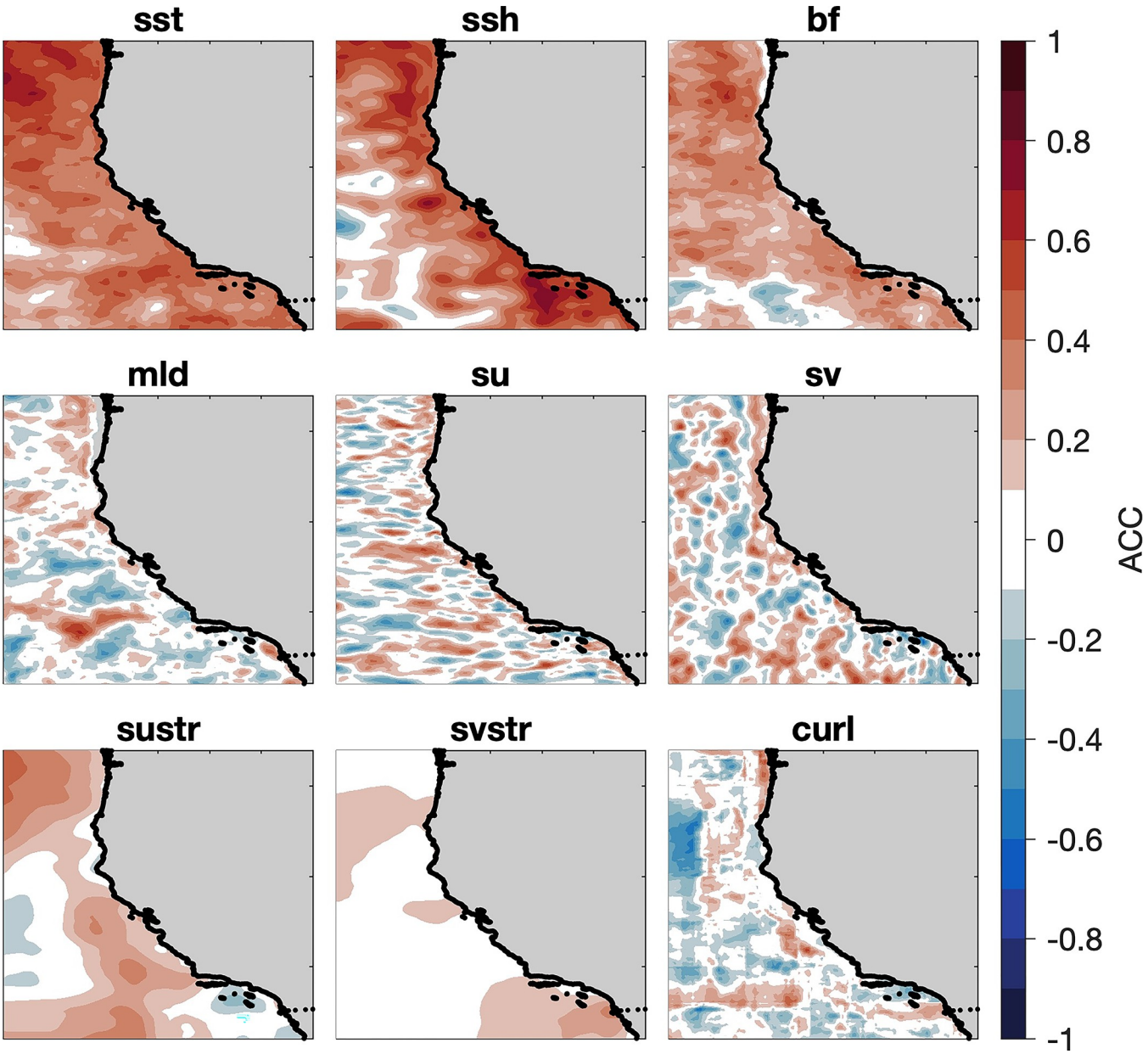

Fig 3. Spatial patterns in forecast skill for oceanic and atmospheric variables. Colors indicate anomaly correlation coefficient for July initialized forecasts at 8.5-month lead (i.e., forecasts of March initialized the prior July). A similar example for January initialized forecasts is shown in S3 Fig. Results are shown for forecasts with bias corrected forcing (i.e., ROMS-CanCM4-BC).

https://doi.org/10.1371/journal.pclm.0000245.g003

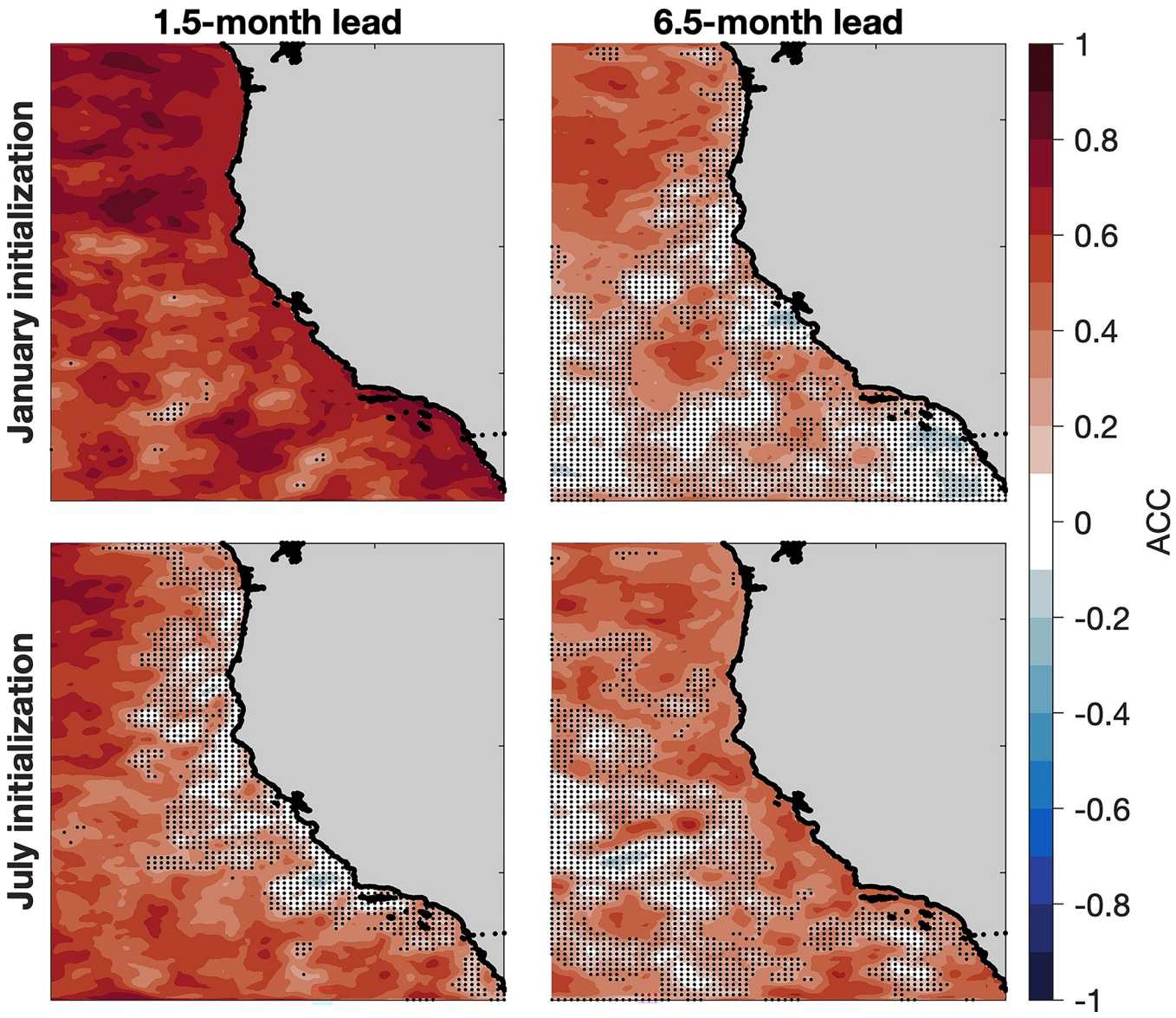

Fig 4. Spatial patterns in SST forecast skill. Colors indicate anomaly correlation coefficient for (top) January and (bottom) July initialized forecast at two lead times. Black stippling indicates regions with forecast skill that is not significantly greater than zero at the 95% confidence level. Results are shown for forecasts with bias corrected forcing (i.e., ROMS-CanCM4-BC).

https://doi.org/10.1371/journal.pclm.0000245.g004

In addition to temporal patterns in forecast skill, spatial structure is also apparent over the CCS domain in both the cross-shore and latitudinal directions (Figs 4–6, S4 Fig). For SST (Fig 4), the nearshore environment is especially unpredictable in summer (e.g., 6.5-month forecasts initialized in January, 1.5-month forecasts initialized in July), while in winter it exhibits relatively high forecast skill (e.g., 6.5-month forecasts initialized in July). As noted above, this coastal predictability in winter is consistent with forcing from ENSO, and it is even more apparent in SSH (Fig 5). The coastal SSH predictability can arise from ENSO's atmospheric teleconnection (through changes in alongshore winds and associated Ekman transport [20]) as well as the oceanic teleconnection (poleward propagation of coastal trapped waves [66]). The latter is also consistent with an alongshore gradient in forecast skill, as the oceanic teleconnection is stronger in

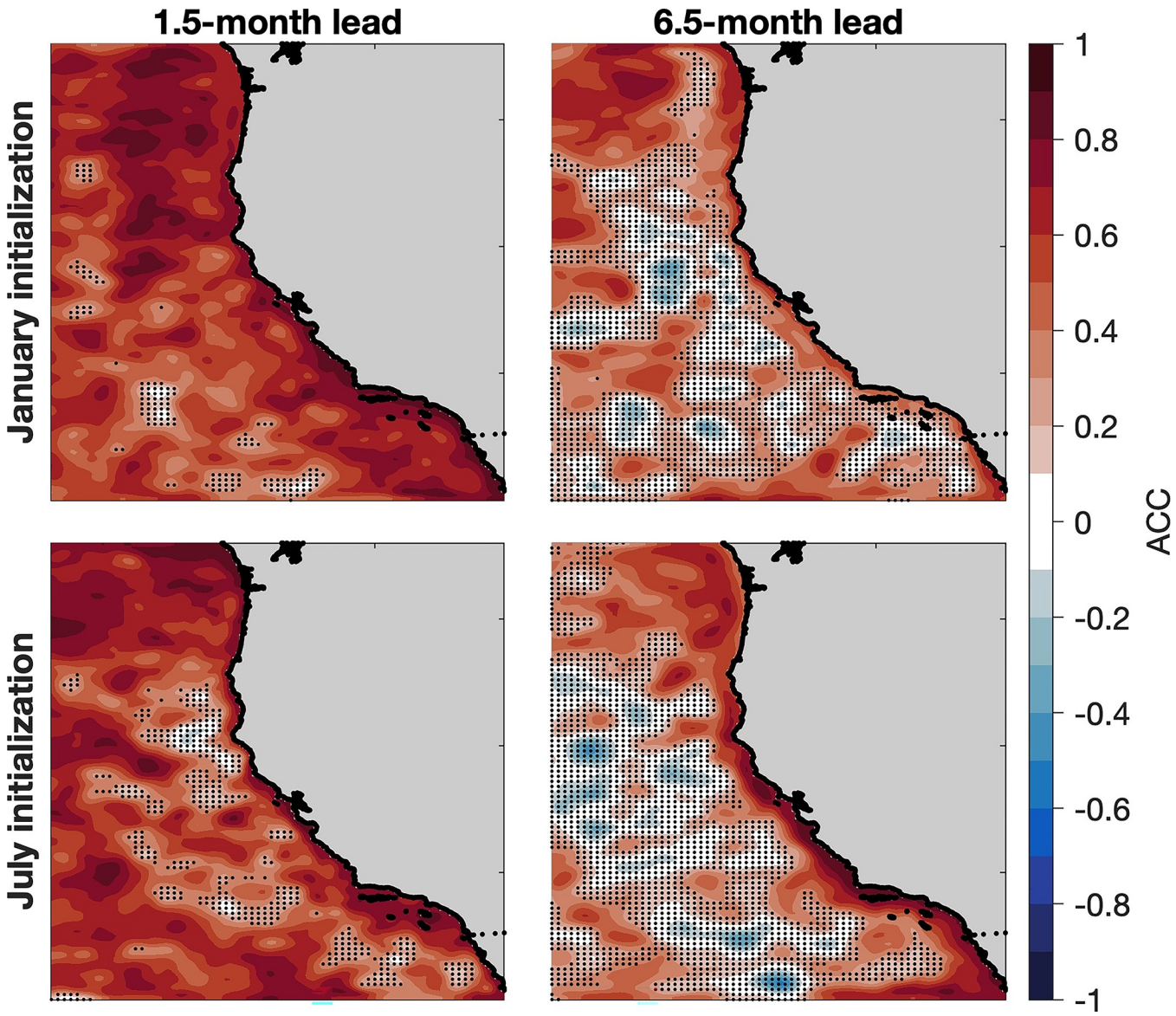

Fig 5. Spatial patterns in SSH forecast skill. As in Fig 4, but for SSH.

https://doi.org/10.1371/journal.pclm.0000245.g005

the southern CCS than it is farther north [67, 68]. While [20] suggested that the atmospheric teleconnection was largely responsible for ENSO-related SST forecast skill in a 10-member global forecast ensemble, here we find that the oceanic teleconnection appears to dominate dynamical forecast skill for a smaller, higher-resolution forecast ensemble (see Section 4). For bottom temperature, short-lead forecast skill is generally higher at deeper depths, likely due to greater persistence, while winter forecasts initialized in July exhibit higher skill at shallower depths (Fig 6).

Shore-based observations of SST and sea level provide additional data sets with which to verify our forecasts. Evaluating the forecasts with these *in situ* datasets leads to patterns in forecast skill similar to those described above (Figs 7 and 8). Specifically, forecasts initialized in January have higher skill at short lead times, forecasts initialized in July have higher skill at longer lead times, and there is a clear latitudinal gradient in SSH forecast skill (e.g., see July-initialized lead 6 forecast in July Fig 8). While these patterns are consistent across verification

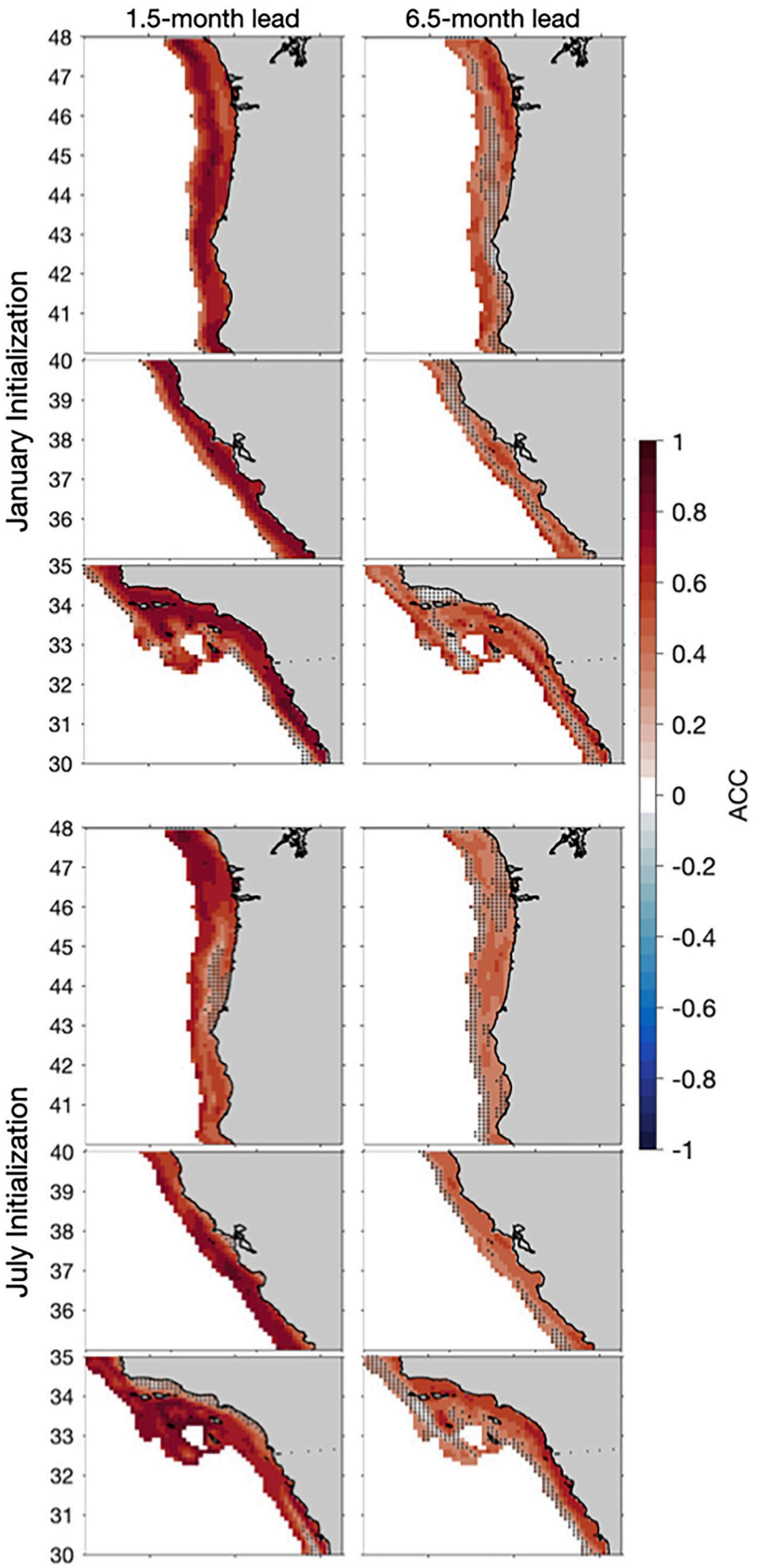
1.5-month lead
6.5-month lead
January Initialization
July Initialization
48
47
46
45
44
43
42
41
40
39
38
37
36
35
34
33
32
31
30
1
0.8
0.6
0.4
0.2
0
-0.2
-0.4
-0.6
-0.8
-1
ACC

Fig 6. Spatial patterns in bottom temperature forecast skill. As in Fig 4, but for bottom temperature. Skill evaluations are limited to regions with bottom depth < 1000 m. Panels are split in the alongshore direction to focus on the nearshore region (latitude is indicated on y-axes).

https://doi.org/10.1371/journal.pclm.0000245.g006

datasets, comparing forecasts to shore-based measurements gives reduced forecast skill (i.e., lower anomaly correlations) and highlights a difference in forecast and observed variance, with forecasts exhibiting lower variability than *in situ* measurements (Figs 7 and 8). These discrepancies likely arise from two key sources. First, model output (from both forecasts and the reanalysis) represents conditions averaged over a 0.1˚ (~10 km x 10 km) box, while shore stations are point measurements and thus can be influenced by very local processes and bathymetric features; these scale differences alone would cause differences even with perfect forecasts. Second, since the forecasts use the same model configuration as the reanalysis (and are initialized from it for CanCM4-ROMS-BC), skill metrics calculated using the reanalysis are likely optimistic. For example, relative to the reanalysis, the CanCM4-ROMS-BC initialization is perfect, but in reality forecasts will be initialized with some errors. This second effect can be explored using alternate gridded data sets for verification, and we find that forecast skill changes little when using OISST or GLORYS for verification rather than CCSRA (S5 and S6 Figs).

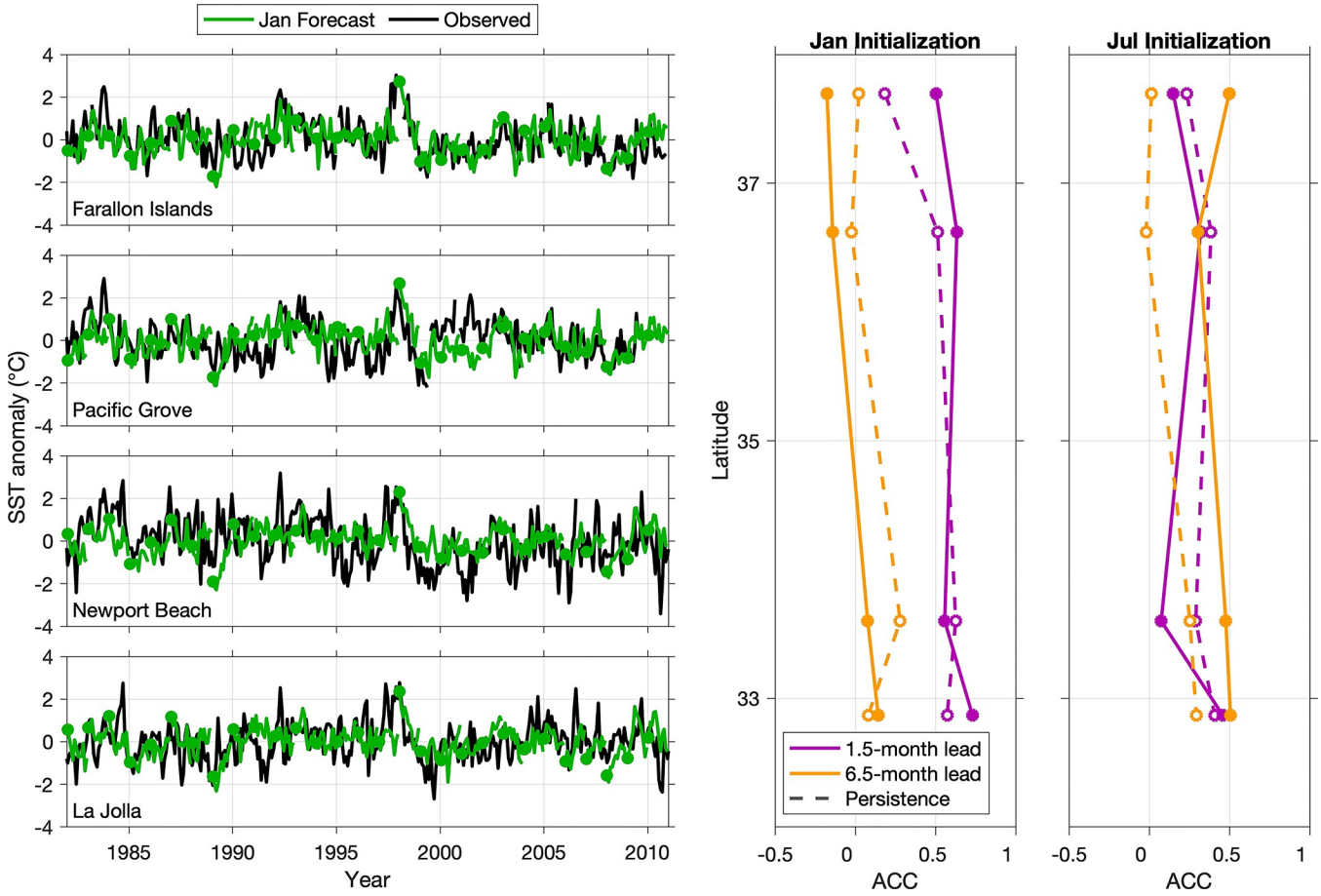

Fig 7. Forecast comparison with coastal SST measurements. (left) time series of observed SST and January initialized forecast SST for 1982–2010 at four locations along the California coast: Farallon Islands (37.7˚N), Pacific Grove, CA (36.6˚N), Newport Beach (33.6˚N), and La Jolla (32.9˚N). Forecast initializations are shown as colored circles. (right) Forecast skill (as measured by anomaly correlation coefficient) for each location as a function of initialization month and lead time. Dashed lines show the skill of persistence forecasts, which serve as a baseline against which model forecast skill can be compared.

https://doi.org/10.1371/journal.pclm.0000245.g007

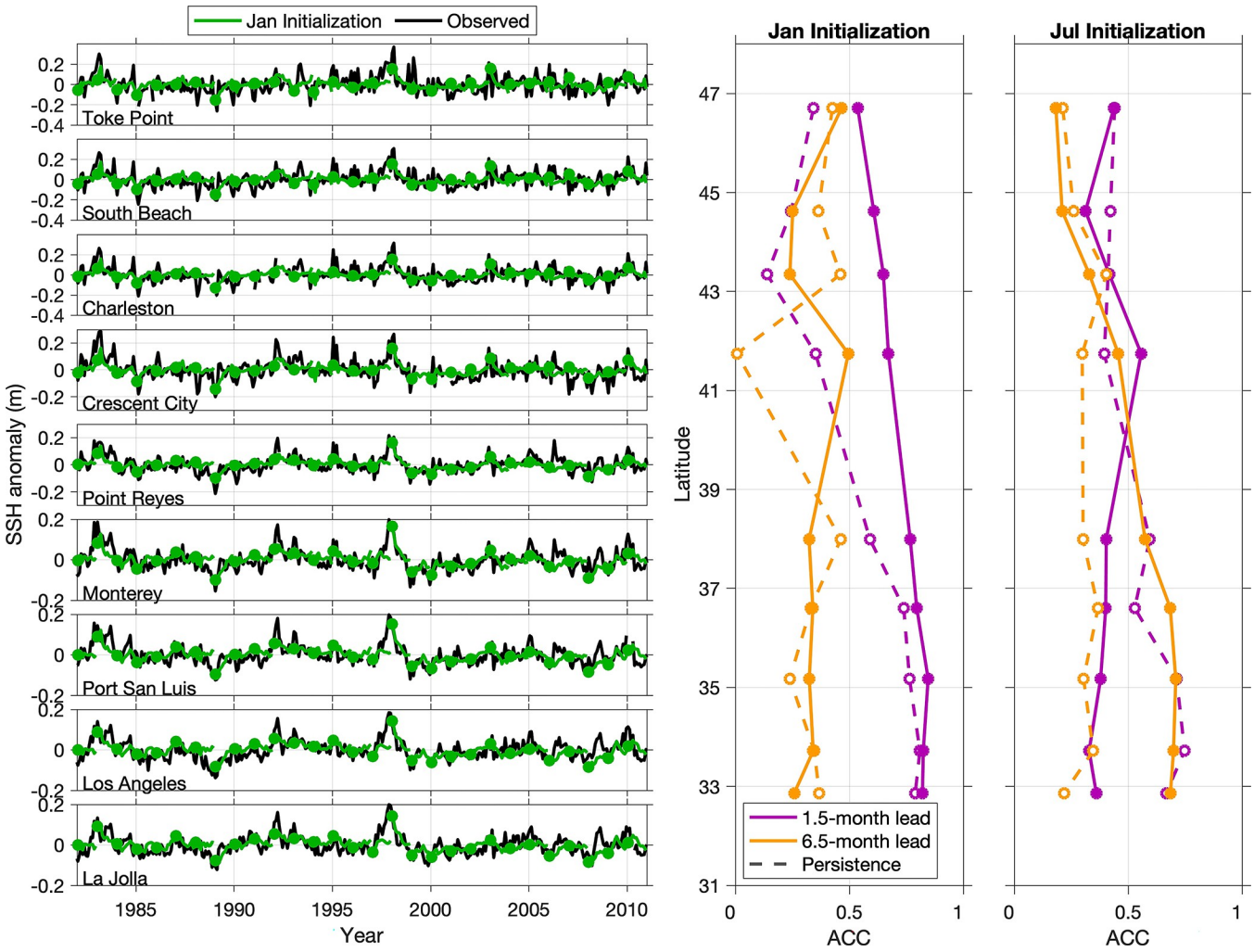

Fig 8. Forecast comparison with coastal sea level measurements. As in Fig 7, but for sea level anomalies at nine tide gauge locations spanning the U.S. west coast: Toke Point, WA (46.7˚N), South Beach, OR (44.6˚N), Charleston, OR (43.3˚N), Crescent City, CA (41.7˚N), Point Reyes, CA (38.0˚N), Monterey, CA (36.6˚N), Port San Luis, CA (35.2˚N), Los Angeles, CA (33.7˚N), and La Jolla, CA (32.9˚N).

https://doi.org/10.1371/journal.pclm.0000245.g008

Given these considerations, the true forecast skill likely falls between the estimates obtained from verification with CCSRA and with the shore-based time series.

3.2. Characteristics of the forecast ensemble

By comparing individual ensemble members, we can glean further information on the uncertainty of forecasts as well as relationships between forecast skill for different variables. Forecast spread (i.e., the difference between the highest and lowest forecasts for a given variable) varies widely throughout the CCS domain, consistent with patterns of variability in the region (Fig 9). For SST, bottom temperature, and stratification, the greatest forecast spread occurs in a narrow coastal band, where high variability coincides with coastal upwelling and relatively shallow bottom depths. In contrast, forecast spread for SSH is greatest several hundred kilometers offshore of California where eddy kinetic energy is at a maximum [69] and forecast skill is relatively poor (Fig 5).

By design, the three CanCM4 forecast members chosen for downscaling vary considerably in their SST forecast skill (see Methods and S1 Fig), and the downscaled forecasts reflect the

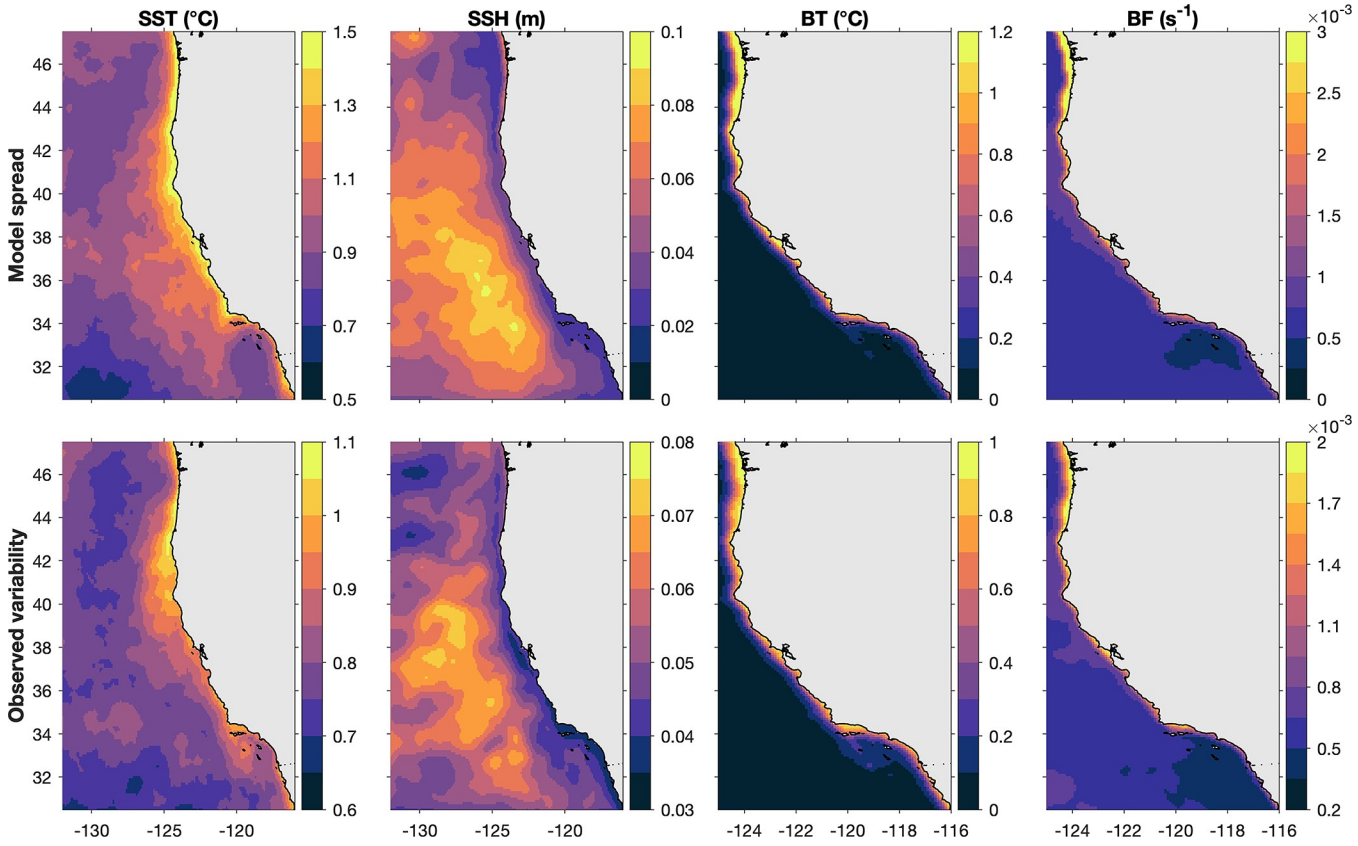

Fig 9. Forecast ensemble spread. (top) Mean spread (i.e., max–min) of the three-member forecast ensemble, averaged across all lead times from the July initialized forecasts, for sea surface temperature (SST), sea surface height (SSH), bottom temperature (BT), and buoyancy frequency (BF). (bottom) Observed variability in these same variables, calculated as the standard deviation of monthly anomalies from the entire study period. Note that scales are different between top and bottom panels, and maps of BT and BF are zoomed into the coast where signals are strongest.

https://doi.org/10.1371/journal.pclm.0000245.g009

skill of the global ensemble members that forced them. Anomaly correlation coefficients for SST, averaged across all lead times and initializations, range from ~0.2 (member 2) to ~0.4 (member 10; Fig 10). The same pattern is also apparent for most other variables, indicating that a forecast that performs relatively well for one aspect of the ocean state (e.g., SST) is likely to also perform relatively well for others (e.g., SSH, bottom temperature, stratification). Furthermore, the skill of the ensemble means tend to be as good as or better than that of the best individual ensemble member. This finding is common in assessments of forecast ensembles (e.g., [17]) and demonstrates the value of including even relatively poorly performing forecasts in the ensemble.

3.3. Influence of bias-corrected forcing

A key methodological decision when forcing regional ocean models with output from global climate models is how to correct for biases in the global model output. One approach is to force the regional model with output that has not been adjusted, simply interpolating the forcing fields to the regional grid (e.g., [9]). Advantages of this method are its relative simplicity and that it maintains dynamical consistency of the forcing fields, with the tradeoff that the downscaled model will inherit biases that need to be accounted for. Alternatively, the global forcing fields can be corrected before running the regional model, with the aim of producing a

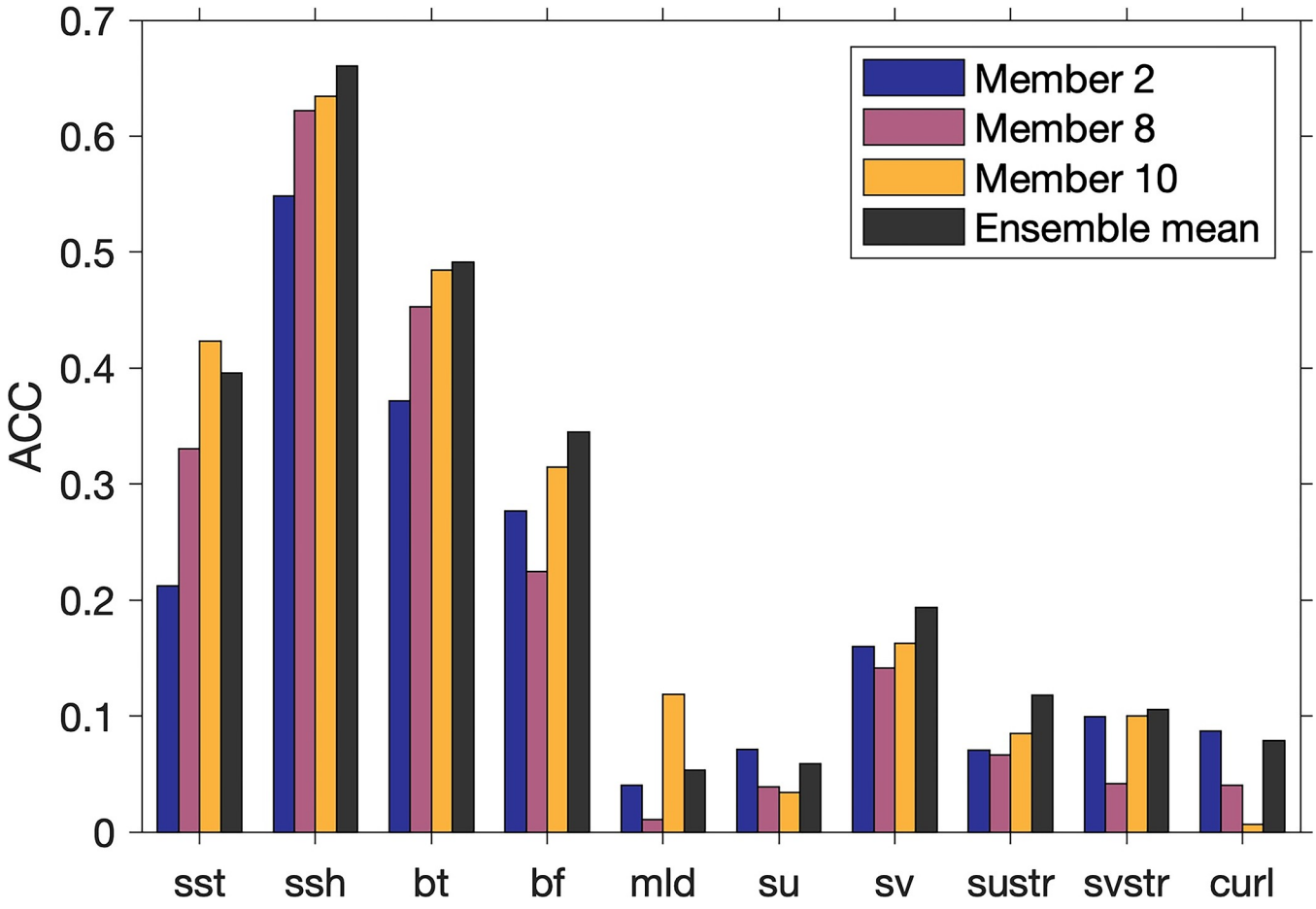

Fig 10. Forecast skill for individual ensemble members and ensemble mean. CanCM4-ROMS-BC skill for each variable is computed in the 75 km wide coastal band extending from 30.5 to 47.5N, and then averaged across all lead times and both initialization months to calculate a mean forecast skill for each variable.

https://doi.org/10.1371/journal.pclm.0000245.g010

more realistic ocean run that does not require post hoc bias correction. Here we employed both approaches to evaluate the implications of choosing one or the other.

Not surprisingly, bias-correcting the global model output tends to reduce bias in the downscaled forecasts (e.g., Fig 1), with the most pronounced impacts seen in bottom temperature, wind stress curl, and meridional wind stress and currents (Fig 11; note that biases in SSH can reflect different reference levels for sea level, not necessarily model performance). However, bias correction can also be performed after downscaling, provided that one can reliably quantify climatological ocean conditions (e.g., with observations or reanalyses). Thus, perhaps of more interest is how the forecast configuration impacts the representation of interannual variability. Comparing CanCM4-ROMS to CanCM4-ROMS-BC, we see that impacts on anomaly forecast skill are generally subtle, though in some cases there do appear to be improvements (see ΔACC and Δforecast accuracy in Fig 11). In particular, the bias-corrected runs benefit from being initialized with the near-real-time regional analysis, generating improved skill especially at shorter lead times. Most notable are improvements in SSH forecasts, as the narrow coastal band most influenced by cross-shore Ekman transport is not resolved in the global model (and therefore in the CanCM4-ROMS run for which initial conditions are interpolated directly from the global model). While these improvements may be inflated due to the

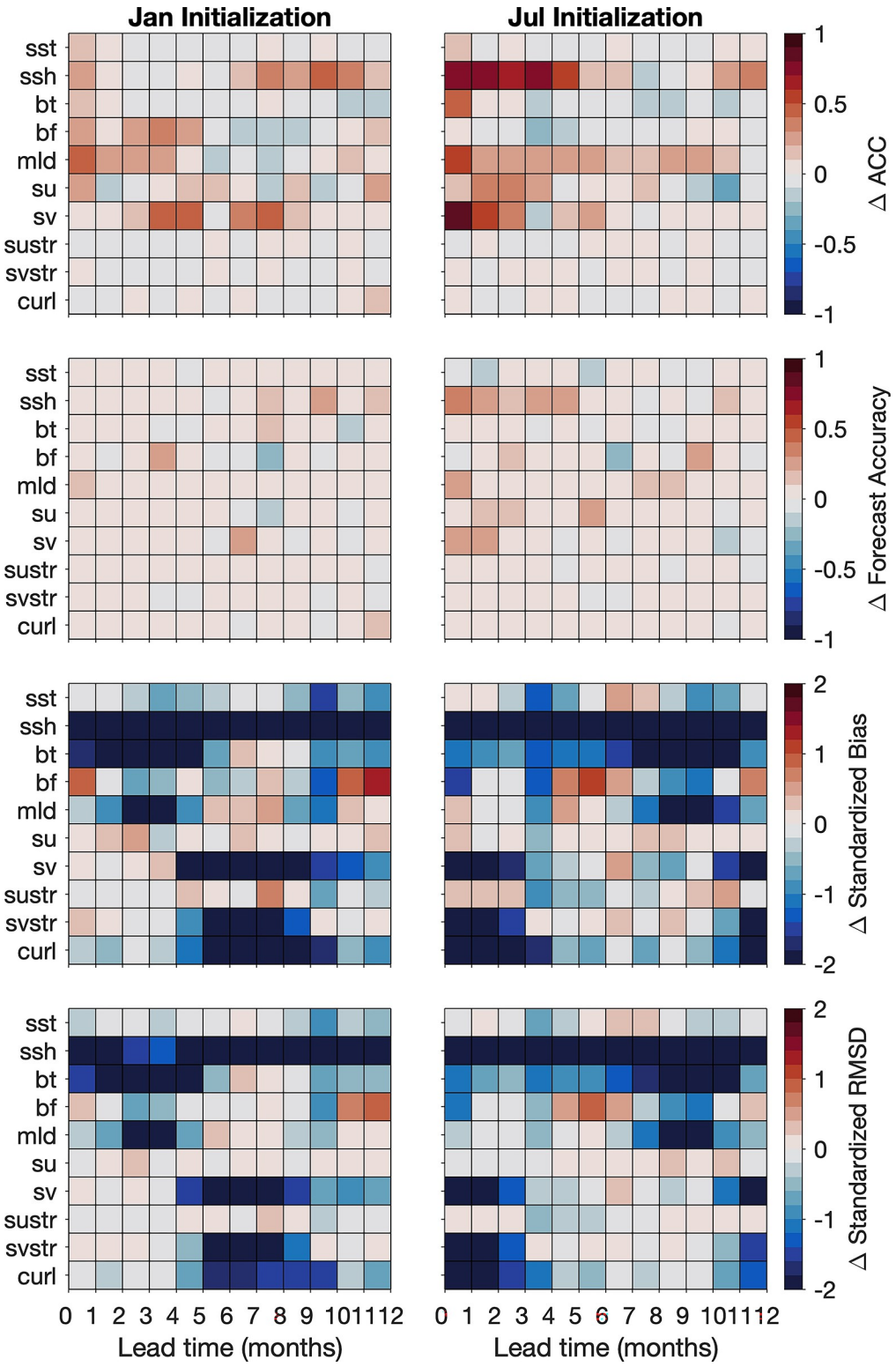

Fig 11. Influence of bias corrected forcing on forecast skill. Differences in skill metrics calculated from forecasts run using bias corrected forcing (CanCM4-ROMS-BC) and those without bias correcting forcing (CanCM4-ROMS) are shown for multiple variables, lead times and initialization months (as in Fig 2). Improvements due to bias correction are indicated by increases (red) for ACC and forecast accuracy, and decreases (blue) for bias and RMSD. Note that bias in SSH can simply reflect differences in the reference for sea level and not necessarily model performance.

https://doi.org/10.1371/journal.pclm.0000245.g011

"perfect" initialization of CanCM4-ROMS-BC relative to the CCSRA verification dataset, the improvements in SSH anomaly forecast skill are confirmed by evaluating both forecast configurations against tide gauge data (not shown).

3.4. Prospects for living marine resource applications

Ultimately, the motivation for developing and evaluating the ocean forecasts described here is to support their broader use, particularly in ecological applications to improve living marine resource management. While we don't explicitly evaluate ecological forecasts here, we can tailor the physical forecast evaluation to specific applications as an initial evaluation of their promise. For a set of potential applications in the CCS (Table 1), the complexity of the required physical forecasts varies widely, with some needing only spatially-averaged SST forecasts for a given season and others requiring a large suite of spatially-explicit oceanographic and atmospheric variables for much of the year. These varying levels of complexity are reflected in our application-specific skill assessment. Forecasts of sardine distribution and recruitment, TOTAL, and the HCI show more potential as they depend solely on SST and/or SSH, which have higher mean skill (ACC = 0.4–0.6) as well as lower spread across the requisite physical forecasts (Fig 12). Mean skill is lower (ACC = 0.2–0.3) and spread is higher for the broad suite of variables, including stratification, mixed layer depth, winds, and currents, required by the albacore distribution, AEI, EcoCast, and WhaleWatch applications. For these applications, some of the underlying forecasts are very skillful (ACC$>$0.8) while others are no better than a random guess (ACC$<$0). The forecast potential for these complex models would increase if they could be parametrized to use a reduced set of more skillful variables (SSH, SST, buoyancy frequency; Fig 12), though in some cases a more parsimonious model may not retain sufficient ecological skill [57].

4. Discussion

The multidecadal set of downscaled ocean reforecasts described herein enables an evaluation of CCS forecast skill, including its dependence on the variable being considered, initialization month, lead time, and location within the CCS. In general, the variables we examined can be separated into groups for which forecast skill was relatively good (SST, SSH, bottom temperature, stratification) or poor (MLD, surface winds, surface currents). Forecast skill is generally higher for the first half of the year than the latter half, with forecasts initialized in January benefitting from strong persistence and forecasts initialized in July benefitting from predictability for late winter/spring conditions that is consistent with the influence of ENSO.

The late winter/spring forecast skill above persistence is most pronounced near the coast, especially for SSH. This skill could arise from tropical-extratropical teleconnections through the atmosphere (i.e., alteration of local winds and heat fluxes [28, 70]) and through the ocean (i.e., poleward propagation of coastal trapped waves [66]). Additional exploratory analyses suggest that the latter mechanism is the domain one driving skill in the regional forecasts. First, SST skill above persistence is more closely related to skill above persistence for SSH (a proxy for the oceanic teleconnection) than for surface wind stress (a proxy for the atmospheric teleconnection), especially in the southern CCS (Fig 13). Second, when evaluating forecasts against the "Wind" and "Ocean" sensitivity runs (see Methods), the total skill above persistence is more strongly associated with the Ocean forcing, indicating that the variability being predicted successfully is largely associated with associated with the oceanic teleconnection (Fig 14).

Beyond quantifying the potential for regional forecasts to predict ecologically-relevant ocean variability in the CCS, we can also shed light on additional considerations for

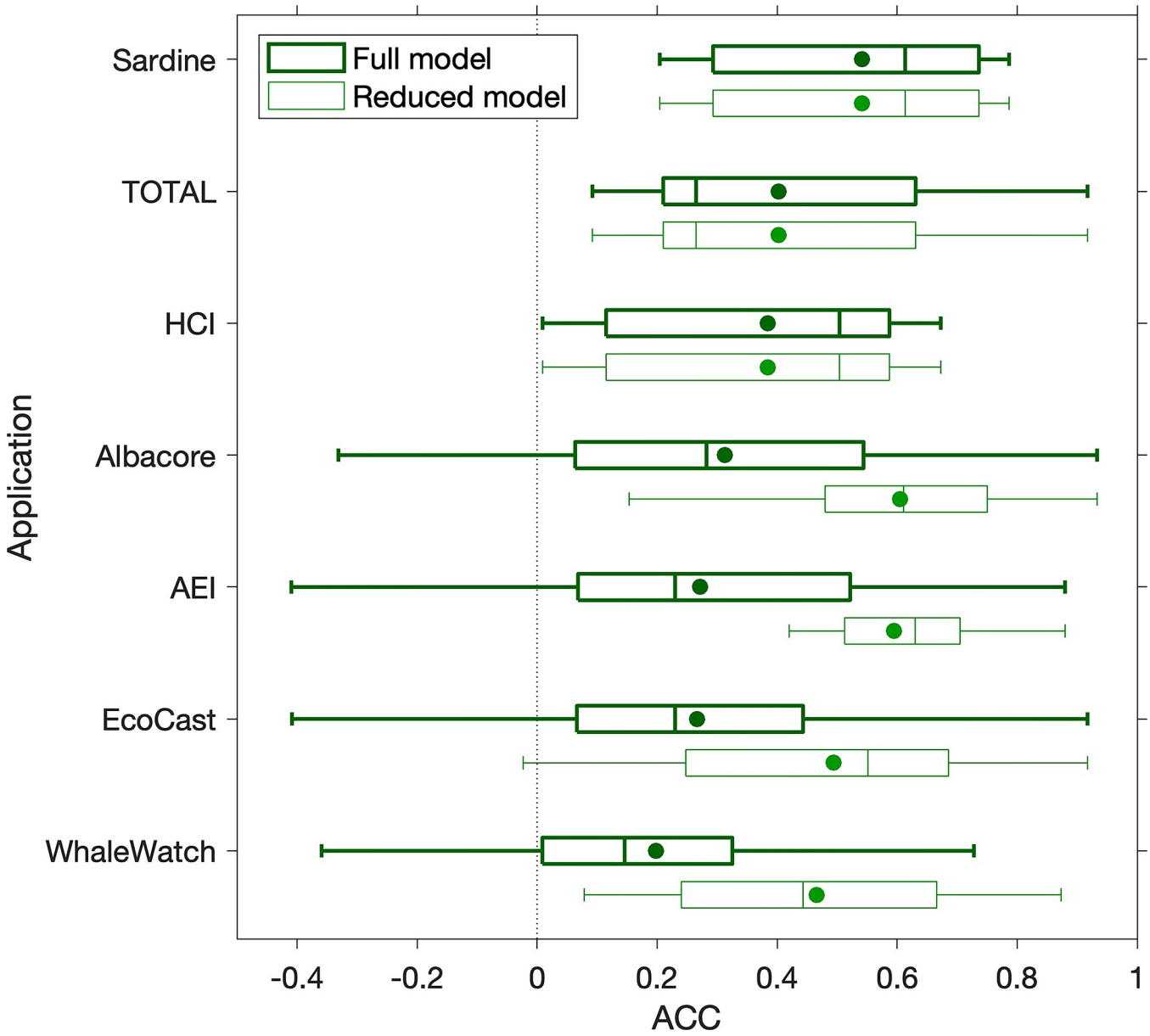

Fig 12. Semi-quantitative skill assessment for potential ecological forecast applications. For each of the potential forecast applications summarized in Table 1, box plots show the range of anomaly correlation coefficients for the variables, months, and regions relevant to that application (see methods). In the reduced models (light green), the same approach is applied but variables are limited to SST, SSH, and buoyancy frequency. Box edges are defined by the 25th and 75th percentiles. Whisker lengths are based on the 1.5 IQR value, i.e., the maximum whisker length is 1.5 times the interquartile range (IQR; difference between 25th and 75th percentiles) and whiskers extend to the most extreme data point within that distance. Medians and means are indicated by vertical lines and filled circles, respectively.

https://doi.org/10.1371/journal.pclm.0000245.g012

operational implementation of such a system. There are now multiple examples of the general approach taken here–linking global climate forecasts to a regional ocean model, which can subsequently drive various types of ecological models [e.g., 9, 10]. Moving such a system from retrospective to real-time applications requires that the necessary forcing fields from the global climate forecast systems be made available in real time, either publicly or in direct collaboration between global and regional modelers. For most global forecast systems, the necessary fields are not readily available, which has been identified as a bottleneck for marine ecosystem

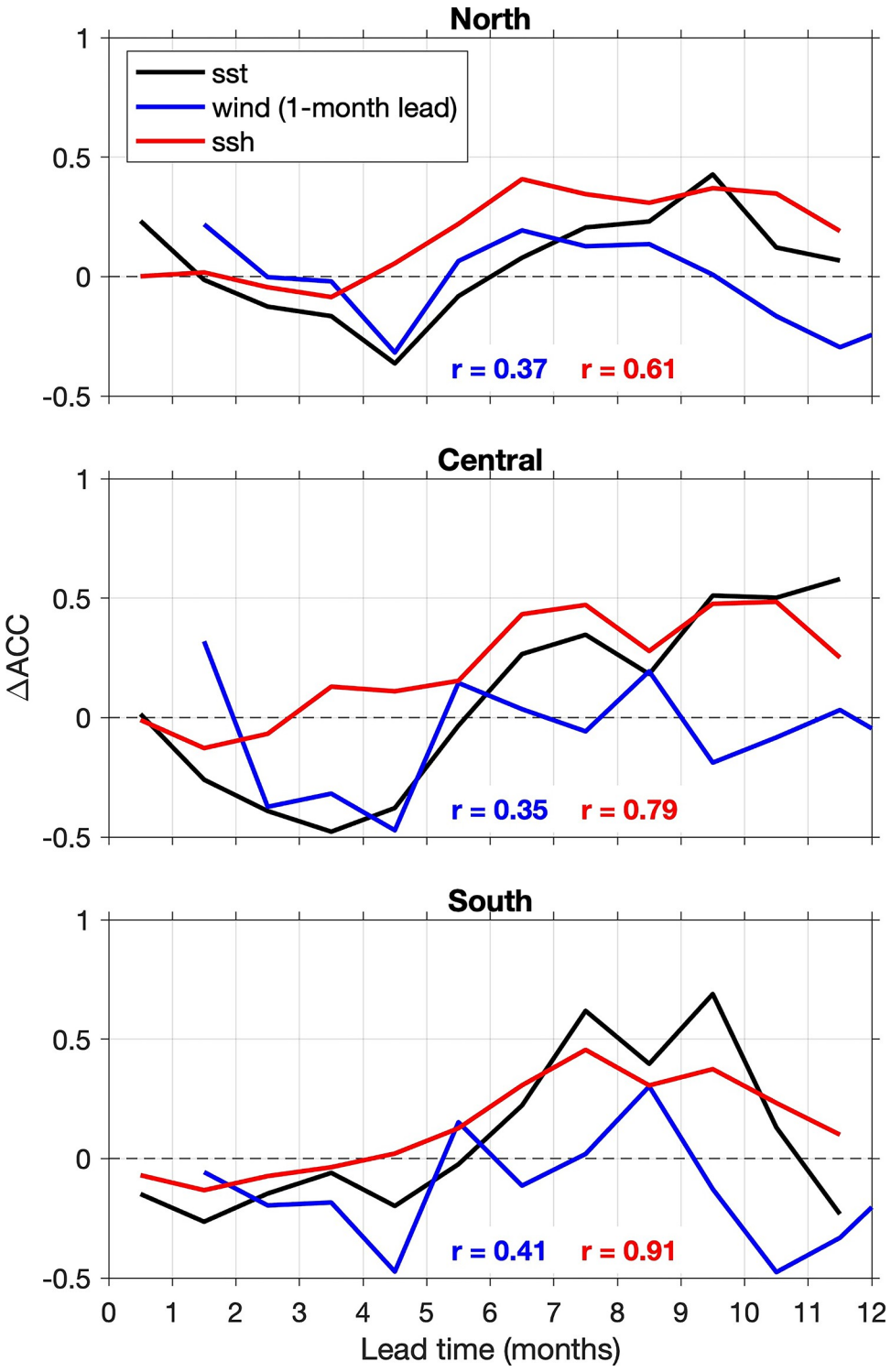

Fig 13. Relationship of skill above persistence for SST, SSH, and surface winds. CanCM4-ROMS-BC minus persistence forecast skill is shown for July-initialized SST, SSH, and surface wind stress forecasts in nearshore (0–75 km) subregions of the CCS. Wind stress skill is the average of skill for the zonal and meridional components (sustr, svstr) and is plotted with one-month lead (i.e., the SST response lags wind by one month). Correlations are shown between SST and wind (blue; proxy for atmospheric teleconnection) and SSH (red; proxy for oceanic teleconnection).

https://doi.org/10.1371/journal.pclm.0000245.g013

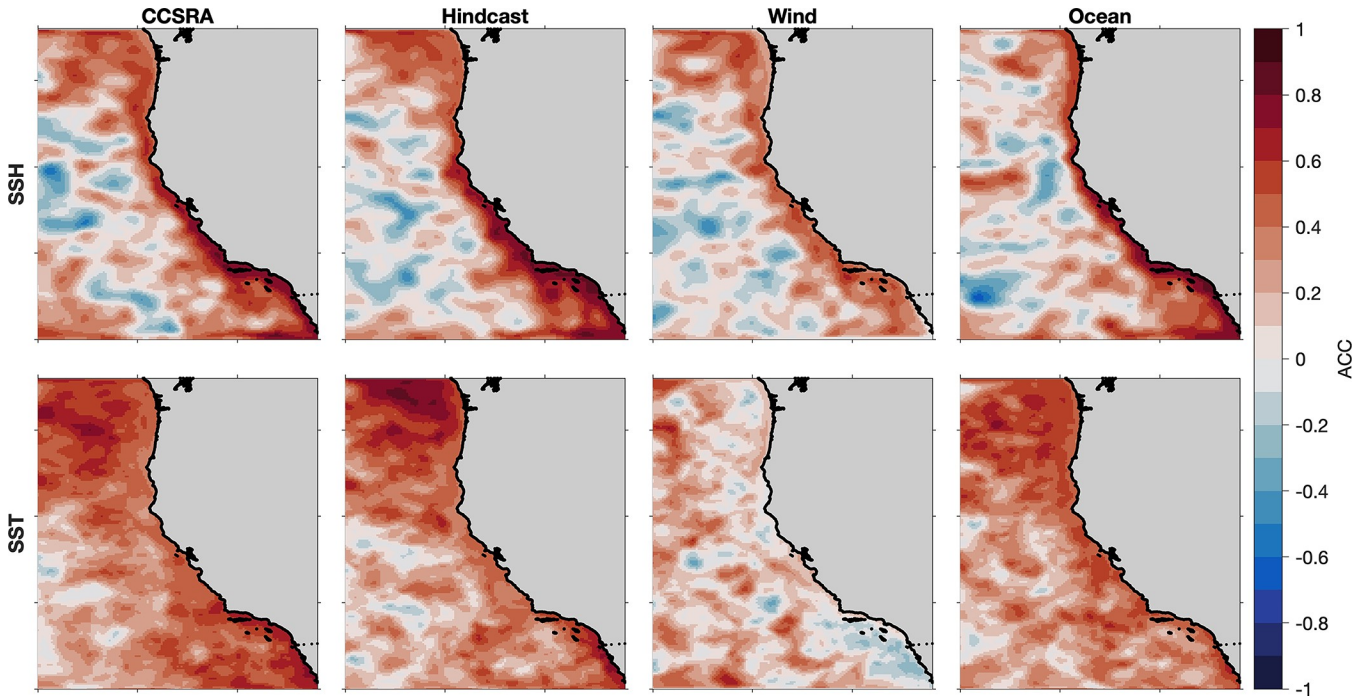

Fig 14. SST forecast skill relative to atmospheric and oceanic forcing. For July-initialized CanCM4-ROMS-BC forecasts at 7.5-month lead, (top) SSH and (bottom) SST forecast skill are shown using different model outputs for verification: the UCSC ocean reanalysis (CCSRA), the Hindcast (like CCSRA but without data assimilation), the Wind run (realistic wind forcing but climatological ocean boundary conditions), and the Ocean run (realistic ocean boundary conditions but climatological winds). Correspondence between the CCSRA and Hindcast shows that verification using the model run without data assimilation still captures forecast skill. Correspondence between the Hindcast and either the Wind or Ocean run shows which forcing mechanism is more closely tied to the model forecast skill.

https://doi.org/10.1371/journal.pclm.0000245.g014

prediction [7]. Once forcing fields are obtained, there are methodological questions regarding bias correction and initialization of the regional model. Our results show that bias correcting the global model output leads to a bias-corrected downscaled forecast. However, an alternate approach is to use the global model output as-is, and bias correct the downscaled forecast output. We found that both methods performed similarly in terms of predicting interannual variability, though slightly higher anomaly correlations for some variables were apparent in the forecasts with bias corrected forcing (Fig 11), which were also initialized from a high-resolution analysis rather than interpolating from the global model. When using this initialization approach, global model output should be bias corrected before running the regional model, so that the boundary conditions are consistent with the initial conditions.

We suggest that physical skill evaluations like the one presented here be used to assess *a priori* the prospects of living marine resource forecasts. For a given application, one can first identify the relevant physical variables, region, and time of year for which forecasts are needed. If these parameters of the ecological forecast align with physical forecast skill, a first condition has been satisfied for a successful prediction. Of course, this assessment is simplified (for example, not explicitly addressing whether an application requires high-resolution spatially resolved conditions or broader area averages; Table 1); however, when trying to identify forecast applications that are likely to be successful, assessments like these provide important insight with relatively little additional investment. According to this physical forecast assessment, the SSH- and SST-based applications (sardine distribution and recruitment, TOTAL, HCI) are the most promising of those explored here. However, when multiple physical variables are used in an application, not all necessarily need to be predicted skillfully in order to

have a useful forecast. For example, a species distribution model built on SST and MLD may derive forecast skill from SST even if MLD anomalies are not predictable. Furthermore, while all variables have been weighted equally in our assessment, they do not contribute equally in the ecological models, where variables such as SST and buoyancy frequency often have relatively high importance. In the examples shown here, albacore distribution, AEI, EcoCast, and WhaleWatch may all derive viable forecast skill from a smaller suite of variables (SST, SSH, buoyancy frequency) despite being built with additional variables that are less predictable.

Of course, successfully predicting physical variability does not guarantee the skill of an ecological forecast, which also depends on the robustness of physical-biological relationships. Such a consideration is exemplified by sardine recruitment, for which the relevant SST forecasts are skillful but the relationship between SST and recruitment has not been robust over time [71]. In some cases, addition of biogeochemistry to the regional forecasts [9] may expand the list of potential ecological applications (e.g., with bottom oxygen concentration for groundfish models or chlorophyll concentration for pelagic species) and allow for more mechanistic underpinning of biological-environmental relationships.

Lastly, an important topic of exploration is the added value of regional downscaling relative to existing global forecasts, from climate models as well as statistical methods [e.g., 63]. While the potential of global forecasts for LMR management has been demonstrated [e.g., 50], there is a desire to resolve ocean variability on fine scales that are known to influence living marine resources. However, regional downscaling comes with considerable computational expense and labor. As a result, downscaled ensembles tend to be relatively small (e.g., 3–6 members) with sparse availability especially in real time, while global forecasts are operationally produced with ensemble sizes of order 100. Given the prominent role of internal climate variability on seasonal forecast timescales, the ability of large global ensembles to adequately represent uncertainty may outweigh the benefits of higher resolution, especially when forecasting rare extreme events [72, 73]. Regional downscaling will likely be more beneficial for fine-scale features like bottom temperature over the shelf or for nearshore biogeochemical processes, and less beneficial for variables like SST that are more strongly constrained by global model forcing. Indeed, for two of the SST-based forecast tools discussed in this paper (TOTAL and HCI), the skill added by downscaling a 3-member ensemble is outweighed by the benefit of using a much larger (~70-member) ensemble of global models [74]. Similarly, the tradeoffs between global and downscaled forecasts are also likely to be regionally dependent, with skill in some regions being more sensitive to resolving fine-scale features, and downscaling will likely to improving some predictive mechanisms than others (e.g., coastal trapped waves vs. large-scale atmospheric anomalies). Thus, when scoping potential regional forecast applications, and when exploring regional ocean prediction more generally, particular attention should be paid to quantifying the added value of downscaling. We argue that marine ecosystem forecasting will benefit from more widely available regional ocean forecasts, but that they are not a prerequisite for many living marine resource forecasts. Rather, the development of new regional forecasting capabilities should be undertaken in parallel with the development and implementation of LMR forecasts that leverage available resources.

Supporting information

S1 Fig. Forecast skill for downscaled ensemble members relative to all CanCM4 ensemble members. (top) SST forecast skill (anomaly correlation coefficient) as a function of lead time for each of the ten CanCM4 ensemble members, highlighting the three members chosen for downscaling in color. (bottom) SST forecast skill for all possible unique 3-member ensembles constructed from the 10-member CanCM4 ensemble (n = 1023; gray lines), with the

downscaled ensemble used for downscaling shown in black.
(JPG)

S2 Fig. Skill summary for downscaled forecasts (ROMS-CanCM4-BC) initialized in (left) January and (right) July of each year, 1982–2010. As in Fig 2, but for a region extending 300 km offshore (Fig 1).
(JPG)

S3 Fig. Spatial patterns in forecast skill for oceanic and atmospheric variables. As in Fig 3, but for January initialized forecasts at 3.5-month lead (i.e., forecasts of April initialized in January).
(JPG)

S4 Fig. Skill summary for downscaled forecasts (ROMS-CanCM4-BC) initialized in (left) January and (right) July of each year, 1982–2010. As in Fig 2, but showing ACC only for north, central, and south subregions.
(JPG)

S5 Fig. Influence of SST verification dataset on forecast skill evaluation. Anomaly correlation coefficient is shown as a function of lead time for SST forecasts evaluated against CCSRA (solid lines) and OISST v2.1 (dashed lines). Skill is shown for both initialization months (January and July) and for three regions, outlined in black on the map at right.
(JPEG)

S6 Fig. Influence of reanalysis verification dataset on forecast skill evaluation. Anomaly correlation coefficient is shown as a function of lead time for SST forecasts evaluated against CCSRA (solid lines) and GLORYS (dashed lines). Variable names are as in Fig 2. Skill is shown for both initialization months (January and July) and for a region extending 75 km offshore and spanning the CCS from 30.5 to 47.5˚N.
(JPEG)

Acknowledgments

Shore station SST data are provided by the Shore Stations Program sponsored at Scripps Institution of Oceanography by California State Parks, Division of Boating and Waterways, Award #C1670003. We thank two anonymous reviewers for feedback to improve the manuscript and Samantha Siedlecki for comments on an early draft of the manuscript.

Author Contributions

Conceptualization: Michael G. Jacox, Stephanie Brodie, Michael A. Alexander, Steven J. Bograd, Christopher A. Edwards, Jerome Fiechter, Elliott L. Hazen, Desiree Tommasi.

Data curation: Michael G. Jacox, Michael A. Alexander, Gaelle Hervieux.

Formal analysis: Michael G. Jacox, Mercedes Pozo Buil, Stephanie Brodie.

Funding acquisition: Michael G. Jacox, Steven J. Bograd, Christopher A. Edwards, Jerome Fiechter, Elliott L. Hazen, Desiree Tommasi.

Investigation: Michael G. Jacox, Mercedes Pozo Buil, Dillon J. Amaya, Desiree Tommasi.

Methodology: Michael G. Jacox, Mercedes Pozo Buil, Stephanie Brodie, Michael A. Alexander, Steven J. Bograd, Gaelle Hervieux.

Project administration: Michael G. Jacox, Michael A. Alexander.

Software: Michael G. Jacox, Mercedes Pozo Buil.

Supervision: Michael G. Jacox.

Validation: Michael G. Jacox.

Visualization: Michael G. Jacox.

Writing – original draft: Michael G. Jacox.

Writing – review & editing: Michael G. Jacox, Mercedes Pozo Buil, Stephanie Brodie, Michael A. Alexander, Dillon J. Amaya, Steven J. Bograd, Christopher A. Edwards, Jerome Fiechter, Elliott L. Hazen, Gaelle Hervieux, Desiree Tommasi.

References

1. Oceanic National and Administration Atmospheric. NOAA Climate, Ecosystems, and Fisheries Initiative. 2021. Retrieved from https://media.fisheries.noaa.gov/2021-08/NOAA%20Climate%20and%20Fisheries%20Initiative%20Fact%20Sheet.pdf
2. Cannizzo ZJ, Selz V. National Marine Sanctuaries Climate Change Science Priorities: Workshop Report. National Oceanographic and Atmospheric Administration, Climate Program Office. 2021. https://doi.org/10.25923/4ftj-3f44
3. Hobday AJ, Spillman CM, Eveson JP, Hartog JR, Zhang X, Brodie S. A framework for combining seasonal forecasts and climate projections to aid risk management for fisheries and aquaculture. Front Mar Sci. 2018; 5:137.
4. Tommasi D, Stock CA, Hobday AJ, Methot R, Kaplan IC, Eveson JP, et al. Managing living marine resources in a dynamic environment: the role of seasonal to decadal climate forecasts. Prog. Oceanogr. 2017; 152:15–49.
5. Payne MR, Hobday AJ, MacKenzie BR, Tommasi D, Dempsey DP, Fässler SM, et al. Lessons from the first generation of marine ecological forecast products. Front Mar Sci. 2017; 4:289.
6. Jacox MG, Alexander MA, Siedlecki S, Chen K, Kwon YO, Brodie S, et al. Seasonal-to-interannual prediction of North American coastal marine ecosystems: Forecast methods, mechanisms of predictability, and priority developments. Prog Oceanogr. 2020; 183:102307.
7. Minobe S, Capotondi A, Jacox MG, Nonaka M, Rykaczewski RR. Toward Regional Marine Ecological Forecasting Using Global Climate Model Predictions From Subseasonal to Decadal Timescales: Bottlenecks and Recommendations. Front Mar Sci. 2022; 9:855965.
8. Drenkard EJ, Stock C, Ross AC, Dixon KW, Adcroft A, Alexander MA, et al. Next-generation regional ocean projections for living marine resource management in a changing climate. ICES J Mar Sci. 2021; 78(6):1969–1987.
9. Siedlecki SA, Kaplan IC, Hermann AJ, Nguyen TT, Bond NA, Newton JA, et al. Experiments with seasonal forecasts of ocean conditions for the northern region of the California Current upwelling system. Sci Rep. 2016; 6(1):1–18.
10. Kearney KA, Alexander M, Aydin K, Cheng W, Hermann AJ, Hervieux G, et al. Seasonal predictability of sea ice and bottom temperature across the eastern Bering Sea Shelf. J Geophys Res Oceans. 2021; 126(11):e2021JC017545.
11. Bograd SJ, Hazen EL, Maxwell S, Leising AW, Bailey H, Brodeur R. Offshore ecosystems. In Mooney H& Zavaleta E(Eds.), Ecosystems of California—A source book (pp. 287–309). Oakland, CA: University of California Press. 2016.
12. Checkley DM, Barth JA. Patterns and processes in the California Current System. Prog Oceanogr. 2009; 83(1–4):49–64.
13. Schwing FB, Bond NA, Bograd SJ, Mitchell T, Alexander MA, Mantua N. Delayed coastal upwelling along the US West Coast in 2005: A historical perspective. Geophys Res Lett. 2006; 33(22).
14. Chavez FP, Collins CA, Huyer A, Mackas DL. El Niño along the west coast of North America, Editorial. Prog. Oceanogr. 2002; 54:1–5.
15. Bond NA, Cronin MF, Freeland H, Mantua N. Causes and impacts of the 2014 warm anomaly in the NE Pacific. Geophys Res Lett. 2015; 42(9):3414–3420.
16. Stock CA, Pegion K, Vecchi GA, Alexander MA, Tommasi D, Bond NA, et al. Seasonal sea surface temperature anomaly prediction for coastal ecosystems. Prog Oceanogr. 2015; 137:219–236.

17. Hervieux G, Alexander MA, Stock CA, Jacox MG, Pegion K, Becker E, et al. More reliable coastal SST forecasts from the North American multimodel ensemble. Clim Dyn. 2019; 53(12):7153–7168.

18. Merryfield WJ, Lee WS, Boer GJ, Kharin VV, Scinocca JF, Flato GM, et al. The Canadian seasonal to interannual prediction system. Part I: Models and initialization. Month Weather Rev, 2013; 141 (8):2910–2945.

19. Kirtman BP, Min D, Infanti JM, Kinter JL, Paolino DA, Zhang Q, et al. The North American multimodel ensemble: phase-1 seasonal-to-interannual prediction; phase-2 toward developing intraseasonal prediction. Bull Am Met Soc. 2014; 95(4):585–601.

20. Jacox MG, Alexander MA, Stock CA, Hervieux G. On the skill of seasonal sea surface temperature forecasts in the California Current System and its connection to ENSO variability. Clim Dyn. 2019; 53 (12):7519–7533.

21. Jacox MG, Tommasi D, Alexander MA, Hervieux G, Stock CA. Predicting the evolution of the 2014–2016 California Current System marine heatwave from an ensemble of coupled global climate forecasts. Front Mar Sci. 2019; 6:497.

22. Veneziani M, Edwards CA, Doyle JD, Foley D. A central California coastal ocean modeling study: 1. Forward model and the influence of realistic versus climatological forcing. J Geophys Res Oceans. 2009; 114(C4).

23. Moore AM, Edwards CA, Fiechter J, Drake P, Neveu E, Arango HG, et al. A 4D-Var analysis system for the California Current: A prototype for an operational regional ocean data assimilation system. In Data Assimilation for Atmospheric, Oceanic and Hydrologic Applications (Vol. II) (pp. 345–366). 2013. Springer, Berlin, Heidelberg.

24. Crawford WJ, Smith PJ, Milliff RF, Fiechter J, Wikle CK, Edwards CA, et al. Weak constraint four-dimensional variational data assimilation in a model of the California Current System, Adv Stat Clim Meteorol Oceanogr. 2016; 2:171–192.

25. Mattern JP, Song H, Edwards CA, Moore AM, Fiechter J. Data assimilation of physical and chlorophyll a observations in the California Current System using two biogeochemical models. Ocean Modell. 2017; 109:55–71.

26. Jacox MG, Moore AM, Edwards CA, Fiechter J. Spatially resolved upwelling in the California Current System and its connections to climate variability. Geophys Res Lett. 2014; 41(9):3189–3196.

27. Jacox MG, Fiechter J, Moore AM, Edwards CA. ENSO and the California Current coastal upwelling response. J Geophys Res Oceans. 2015; 120(3):1691–1702.

28. Jacox MG, Bograd SJ, Hazen EL, Fiechter J. Sensitivity of the California Current nutrient supply to wind, heat, and remote ocean forcing. Geophys Res Lett. 2015; 42(14):5950–5957.

29. Drake PT, Edwards CA, Morgan SG, Dever EP. Influence of larval behavior on transport and population connectivity in a realistic simulation of the California Current System. J Mar Res. 2013; 71:317–350.

30. Brodie S, Jacox MG, Bograd SJ, Welch H, Dewar H, Scales KL, et al. Integrating dynamic subsurface habitat metrics into species distribution models. Front Mar Sci. 2018; 5:219.

31. Becker EA, Carretta JV, Forney KA, Barlow J, Brodie S, Hoopes R, et al. Performance evaluation of cetacean species distribution models developed using generalized additive models and boosted regression trees. Ecol evol. 2020; 10(12):5759–5784. https://doi.org/10.1002/ece3.6316 PMID: 32607189

32. Muhling BA, Brodie S, Smith JA, Tommasi D, Gaitan CF, Hazen EL, et al. Predictability of species distributions deteriorates under novel environmental conditions in the California Current System. Front Mar Sci. 2020; 7:589.

33. Hersbach H, Bell B, Berrisford P, Hirahara S, Horányi A., Muñoz-Sabater J, et al. The ERA5 global reanalysis. Q J R Meteorol. 2020; 146(730):1999–2049.

34. Carton JA, Giese BS. A Reanalysis of Ocean Climate Using Simple Ocean Data Assimilation (SODA). Mon Weather Rev. 2008; 136(8):2999–3017.

35. Neveu E, Moore AM, Edwards CA, Fiechter J, Drake PT, Jacox MG, et al. A historical analysis of the California Current using ROMS 4D-Var. Part I: System configuration and diagnostics, Oce Modell. 2016; 99:133–151.

36. Kara AB, Rochford PA, Hurlburt HE. An optimal definition for ocean mixed layer depth. J Geophys Res Oceans. 2000; 105(C7):16803–21.

37. Anderson CR, Berdalet E, Kudela RM, Cusack CK, Silke J, O'Rourke E, et al. Scaling up from regional case studies to a global harmful algal bloom observing system. Front Mar Sci. 2019; 6:250.

38. Cimino MA, Santora JA, Schroeder I, Sydeman W, Jacox MG, Hazen EL, et al. Essential krill species habitat resolved by seasonal upwelling and ocean circulation models within the large marine ecosystem of the California Current System. Ecography, 2020; 43(10):1536–1549.

39. Abrahms B, Welch H, Brodie S, Jacox MG, Becker EA, Bograd SJ, et al. Dynamic ensemble models to predict distributions and anthropogenic risk exposure for highly mobile species. Divers Distrib. 2019; 25 (8):1182–1193.

40. Schroeder ID, Santora JA, Moore AM, Edwards CA, Fiechter J, Hazen EL, et al. Application of a data-assimilative regional ocean modeling system for assessing California Current System ocean conditions, krill, and juvenile rockfish interannual variability. Geophys Res Lett. 2014; 41(16):5942–5950.

41. Amaya DJ, Alexander MA, Scott JD, Jacox MG. An evaluation of high-resolution ocean reanalyses in the California Current System. Prog Oceanogr. 2023; 210:102951.

42. Amaya DJ, Jacox MG, Alexander MA, Scott JD, Deser C, Capotondi A, et al. Bottom marine heatwaves along the continental shelves of North America. Nat Commun. 2023; 14(1):1038. https://doi.org/10.1038/s41467-023-36567-0 PMID: 36914643

43. Reynolds RW, Smith TM, Liu C, Chelton DB, Casey KS, Schlax MG. Daily high-resolution-blended analyses for sea surface temperature. J Clim. 2007; 20:5473–5496.

44. Banzon V, Smith TM, Chin TM, Liu C, Hankins W. A long-term record of blended satellite and in situ sea-surface temperature for climate monitoring, modeling and environmental studies. Earth Syst Sci Data. 2016; 8:165–176.

45. Caldwell PC, Merrifield MA, Thompson PR. Sea level measured by tide gauges from global oceans—the Joint Archive for Sea Level holdings (NCEI Accession 0019568), Version 5.5, NOAA National Centers for Environmental Information, Dataset, 2015. https://doi.org/10.7289/V5V40S7W

46. Tommasi D, Stock CA, Alexander MA, Yang X, Rosati A, Vecchi GA. Multi-annual climate predictions for fisheries: an assessment of skill of sea surface temperature forecasts for large marine ecosystems. Front Mar Sci. 2017; 4, 201.

47. Wilks DS. Statistical methods in the atmospheric sciences. Academic press. 2011.

48. Bretherton CS, Widmann M, Dymnikov VP, Wallace JM, Bladé I. The effective number of spatial degrees of freedom of a time-varying field. J Clim. 1999; 12:1990–2009.

49. Zwolinski JP, Emmett RL, Demer DA. Predicting habitat to optimize sampling of Pacific sardine (Sardinops sagax). ICES J Mar Sci. 2011; 68:867–879.

50. Tommasi D, Stock CA, Pegion K, Vecchi GA, Methot RD, Alexander MA, et al. Improved management of small pelagic fisheries through seasonal climate prediction. Ecol App. 2017; 27(2):378–388. https://doi.org/10.1002/eap.1458 PMID: 28221708

51. Welch H, Hazen EL, Briscoe DK, Bograd SJ, Jacox MG, Eguchi T. Environmental indicators to reduce loggerhead turtle bycatch offshore of Southern California. Ecol Indic. 2019; 98:657–664.

52. Santora JA, Mantua NJ, Schroeder ID, Field JC, Hazen EL, Bograd SJ, et al. Habitat compression and ecosystem shifts as potential links between marine heatwave and record whale entanglements. Nature commun. 2020; 11(1):1–12. https://doi.org/10.1038/s41467-019-14215-w PMID: 31988285

53. Schroeder ID, Santora JA, Mantua N, Field JC, Wells BK, Hazen EL, et al. Habitat compression indices for monitoring ocean conditions and ecosystem impacts within coastal upwelling systems. Ecol Indic. 2022; 144:109520.

54. Muhling BA, Brodie S, Jacox M, Snodgrass O, Dewar H, Tommasi D, et al. Dynamic habitat use of albacore and their primary prey species in the California current system. Calif Coop Oceanic Fish Invest Rep. 2019; 60:1–15.

55. Fennie HW, Seary R, Muhling BA, Bograd SJ, Brodie S, Cimino MA, et al. An anchovy ecosystem indicator of marine predator foraging and reproduction. Proc. R. Soc. B. 2023; 290(1992). https://doi.org/10.1098/rspb.2022.2326 PMID: 36750186

56. Hazen EL, Scales KL, Maxwell SM, Briscoe DK, Welch H, Bograd SJ, et al. A dynamic ocean management tool to reduce bycatch and support sustainable fisheries. Sci. Adv. 2018; 4(5):eaar3001. https://doi.org/10.1126/sciadv.aar3001 PMID: 29854945

57. Hazen EL, Palacios DM, Forney KA, Howell EA, Becker E, Hoover AL, et al. WhaleWatch: a dynamic management tool for predicting blue whale density in the California Current. J Appl Ecol. 2017; 54 (5):1415–1428.

58. Kaplan IC, Williams GD, Bond NA, Hermann AJ, Siedlecki SA. Cloudy with a chance of sardines: forecasting sardine distributions using regional climate models. Fish Oceanogr. 2016; 25(1):15–27.

59. Malick MJ, Siedlecki SA, Norton EL, Kaplan IC, Haltuch MA, Hunsicker ME, et a. Environmentally driven seasonal forecasts of Pacific hake distribution. Front Mar Sci. 2020; 7:578490.

60. Norton EL, Siedlecki S, Kaplan IC, Hermann AJ, Fisher JL, Morgan CA, et al. The importance of environmental exposure history in forecasting Dungeness crab megalopae occurrence using J-SCOPE, a high-resolution model for the US Pacific Northwest. Front Mar Sci. 2020; 7:102.

61. Norton EL, Kaplan IC, Siedlecki S, Hermann AJ, Alin SR, Newton J, et al. Seasonal ocean forecasts to improve predictions of Dungeness crab catch rates, co-developed with state and tribal fishery managers. ICES J Mar Sci. 2023; fsad010. https://doi.org/10.1093/icesjms/fsad010

62. DeMott C, Muñoz ÁG, Roberts CD, Spillman CM, Vitart F. The benefits of better ocean weather forecasting. Eos. 2021; 102.

63. Shin SI, Newman M. Seasonal Predictability of Global and North American Coastal Sea Surface Temperature and Height Anomalies. Geophys Res Lett. 2021; 48:e2020GL091886.

64. Ray S, Siedlecki SA, Alexander MA, Bond NA, Hermann AJ. Drivers of subsurface temperature variability in the Northern California Current. J Geophys Res Oceans. 2020; 125(8):e2020JC016227.

65. Ray S, Bond N, Siedlecki S, Hermann AJ. Influence of Winter Subsurface on the Following Summer Variability in Northern California Current System. J Geophys Res Oceans. 2022; 127(12): e2022JC018577.

66. Amaya DJ, Jacox MG, Dias J, Alexander MA, Karnauskas KB, Scott JD, et al. Subseasonal-to-Seasonal Forecast Skill in the California Current System and Its Connection to Coastal Kelvin Waves. J Geophys Res Oceans. 2022; 127(1):e2021JC017892.

67. Hermann AJ, Curchitser EN, Haidvogel DB, Dobbins EL. A comparison of remote vs. local influence of El Niño on the coastal circulation of the northeast Pacific. Deep Sea Res Part II. 2009; 56(24):2427–2443.

68. Frischknecht M, Munnich M, Gruber N. Remote versus local influence of ENSO on the California Current System. J. Geophys. Res. Oceans. 2015; 120:1353–1374.

69. Capet X, Colas F, McWilliams JC, Penven P, Marchesiello P. Eddies in eastern boundary subtropical upwelling systems. Ocean Modeling in an Eddying Regime. 2008; 177:131–147.

70. Alexander MA, Bladé I, Newman M, Lanzante JR, Lau NC, Scott JD. The atmospheric bridge: The influence of ENSO teleconnections on air–sea interaction over the global oceans. J Clim. 2002; 15 (16):2205–2231.

71. Zwolinski JP, Demer DA. Re-evaluation of the environmental dependence of Pacific sardine recruitment. Fish Res. 2019; 216:120–125.

72. Doi T, Behera SK, Yamagata T. Merits of a 108-member ensemble system in ENSO and IOD predictions. J Clim. 2019; 32(3):957–972.

73. Jacox MG, Alexander MA, Amaya D, Becker E, Bograd SJ, Brodie S, et al. Global seasonal forecasts of marine heatwaves. Nature. 2022; 604(7906):486–490. https://doi.org/10.1038/s41586-022-04573-9 PMID: 35444322

74. Brodie S, Pozo Buil M, Welch H, Bograd SJ, Hazen EL, Santora JA, et al. Ecologicall forecasts for marine resource management during climate extremes. Nature commun. 2023. In press.